Stratigraphy and palaeoenvironment of the early Jurassic volcaniclastic strata at Djupadalsmölla, central Skåne, Sweden

PER WAHLQUIST

Dissertations in Geology at Lund University,
Master's thesis, no 646
(45 hp/ECTS credits)

Department of Geology
Lund University
2023

Stratigraphy and palaeoenvironment of the early Jurassic volcaniclastic strata at Djupadalsmölla, central Skåne, Sweden

Master's thesis

PER WAHLQUIST

Department of Geology
Lund University
2023

Contents

Cover Picture: Landscape recreation based on the the view from across the Rönne river from the Djupadalsmölla deposit. By Anna Kurop 2022.

Stratigraphy and palaeoenvironment of the early Jurassic volcaniclastic strata at Djupadalsmölla, central Skåne, Sweden

PER WHLQUIST

Wahlquist, P., 2023: Stratigraphy and palaeoenvironment of the early Jurassic volcaniclastic strata at Djupadalsmölla, central Skåne, Sweden. *Dissertations in Geology at Lund University*, No. 646, 33 pp. 45 hp (45 ECTS credits).

Abstract: From the almost 200 volcanic outcrops in the Central Skåne Volcanic Province (CSVP), only three are of volcaniclastic material. These volcanoclastics, and the transition to the underlying crystalline basement, have been investigated for the first time in a drill core (KBH2) from Djupadalsmölla in order to understand the stratigraphy, depositional process, age of deposition, and depositional environment. The core constitutes three rock units, in ascending order: the kaolinite weathered crystalline basement, a thin dark coloured mudstone, and a massive lapilli tuff (volcaniclastics). From the degraded state of the crystalline basement, it is clear that extensive chemical weathering tock place implying a wet and humid climate. Through palynological studies of the mudstone unit the depositional environment was likely a restricted bay or lagoon with limited marine influences surrounded by a forest covered wetland at the time of volcanism. The age of the mudstone could be determined to late Pliensbachian through the palynomorphs. Petrographic analysis shows that all but the lowermost part of the volcaniclastic deposit has a lapilli tuff texture. The material is, however, highly degraded and replaced by swelling clay minerals and highly affected by diagenetic processes. The depositional process could only be narrowed down to two alternatives. Either directly deposited by a pyroclastic flow or secondarily deposited by a lahar.

Keywords: volcaniclastic, Djupadalsmölla, CSVP, palynomorphs, early Jurassic, late Pliensbachian,

Supervisor: Mikael Calner

Co-supervisors: Ulf Söderlund, Sofie Lindström, Oliver Lehnert and Carita Augustsson

Subject: Bedrock Geology

Per Wahlquist, Department of Geology, Lund University, Sölvegatan 12, SE-223 62 Lund, Sweden. E-mail: Peroristen@gmail.com

Stratigrafi och paleomiljö av tidig jurassisk vulkanoklastisk strata vid Djupadalsmölla i centrala Skåne

PER WAHLQUIST

Wahlquist, P., 2023: Stratigrafi och petrografi av tidig jurassisk vulkanoklastisk strata vid Djupadalsmölla i centrala Skåne. *Examensarbeten i geologi vid Lunds universitet*, Nr. 646, 33 sid. 45 hp.

Sammanfattning: Av de nästan 200 blottningarna av vulkaniska bergarter som kan ses i Central Skåne Volcanic Province (CSVP) består endast tre av vulkanoklastiskt material. Stratigrafin i dessa avlagringar vars förhållande till underliggande urberg har för första gången beskrivits i en borrkärna (KBH2) från Djupadalsmölla för att bestämma stratigrafin samt avsättningsprocessen, åldern och avsättningsmiljön. Borrkärnan består av tre enheter i stigande ordning: det kaolinitvitrade kristallina urberget, den mörka lerstenen, och den massiva lapilli tuffen (vulkanoklastisk). Utifrån urbergets vittrade tillstånd står det klart att utbredd kemisk vittring ägde rum vilket tyder på ett mycket blött och fuktigt klimat. Palynologiska studier av lerstenen tyder på att avsättningsmiljön var en avgränsad marin vik eller lagun i ett annars skogsklätt landskap när vulkanismen ägde rum. Åldern på lerstenen kunde också bestämmas till sen Pliensbachian utifrån de palynologiska studierna. Petrografisk analys visade att allt utom den allra nedersta delen av det vulkanoklastiska materialet påvisas ha en lapilli tuff textur, dock är det klart att materialet är mycket nedbrutet och ersatt av svällande lermineral men även starkt påverkade av diagenetiska processer. Den exakta avsättningsprocessen kunde inte identifieras men två alternativ kunde nås. Antigen direktavsatt från ett pyroklastiskt flöde eller en sekundärt avsatt av en lahar.

Nyckelord: volcanoklastiskt, Djupadalsmölla, CSVP, palynomorpher, tidig Jura, sen Pliensbachian,

Handledare: Mikael Calner

Medhandledare: Ulf Söderlund, Sofie Lindström, Oliver Lehnert and Carita Augustsson

Ämnesinriktning: Berggrunds Geologi

Per Wahlquist, Geologiska institutionen, Lund University, Sölvegatan 12, SE-223 62 Lund, Sweden. E-post: Peroristen@gmail.com

1 Introduction

Volcanic rocks are relatively common in certain areas of Sweden, and some of these are associated with mineral deposits. These rocks are generally Proterozoic in age, >1.8 Ga, and located in central (Bergslagen area) and northern (Skellefteå region) Sweden (Salin et al. 2021). In the southernmost province of Sweden, i.e., Skåne, the youngest known volcanic remnants in the entire country are found (Fig. 1). These are represented by more than one hundred outcrops of basaltic rocks and include at least three outcrops with poorly consolidated volcaniclastic rocks (Wikman et al. 1993; Wikman & Sivhed 1993; Augustsson 2001). These basaltic and volcaniclastic rocks are concentrated within an area of 1200 km2 in the central part of Skåne, which Vajda et al. (2016) referred to as the Central Skåne Volcanic Province (CSVP). The ages of the rocks have been dated to early Jurassic to early Cretaceous using a variety of dating techniques (Tralau 1973; Bylund & Halvorsen 1993; Bergelin 2009; Bergelin et al. 2010; Tappe et al. 2016; Vajda et al. 2016). Ar-Ar geochronological studies suggest at least three pulses of volcanism dated at 191-176 Ma, 145 Ma and 110 Ma (Bergelin et al. 2010).

The aim of this study is to describe and document the volcaniclastic rocks from a drill core recovered at Djupadalsmölla in central Skåne (Bergelin & Calner 2012; Fig. 1). This is the only known drill core (KBH2) comprising volcaniclastic rocks from the CSVP. I have performed detailed logging and documentation of the core as well as studied the petrography in order to investigate depositional processes and the origin of lithic material within the deposit. In addition, I have analysed palynological data to date the rocks, and to interpret the plausible paleoenvironment at the time of deposition. The latter also required description of the rock units immediately underlying the volcaniclastic deposits.

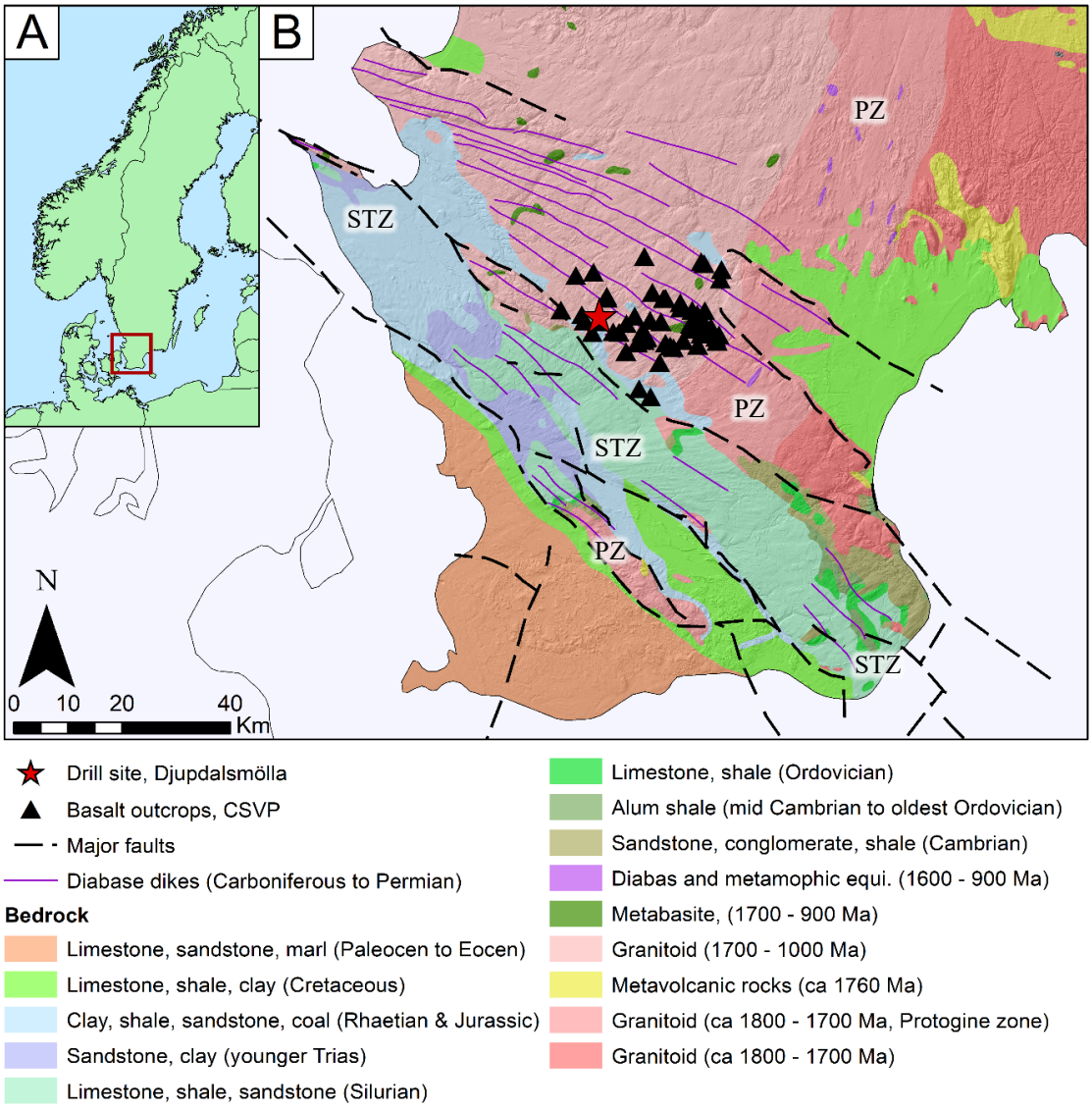

Figure 1. A) Location of map B in the southern-most province of Sweden, Skåne. B) Geological map of Skåne superimposed on the topographical map, showing the main tectonic units and major fault lines. Note the position of the Central Skåne Volcanic Province (CSVP) near the intersection of the north-south-trending Protogine Zone (PZ) and the southeast-northwest-trending Sorgenfrei-Tornquist Zone (STZ). The drill site at Djupadalsmölla is marked by the red star. Map data: Lantmäteriet© & SGU©.

1.1 Earlier research

Basaltic and pyroclastic rocks of the CSVP were identified as being of volcanic origin first in the early 19th century (Hisinger 1826), and the first scientific documentations of these rocks were made in the 1870's and 1880's (Tullberg & Nathorst 1880; Eichstädt 1883; Svedmark 1883; Wikman & Sivhed 1993). Over the following 75 years only a few works on the CSVP were conducted (Henning 1902; Norin 1934; Norin 1940). In the 1950's and 1960's a series of studies on the basalts and volcaniclastic deposits were published, but the age of the volcanism was still uncertain. From wooden logs enclosed in the volcaniclastic deposits, a Cenozoic age had been suggested in the late 20th century (Printzlau & Larsen 1972). The age span of these fossils was later revised and is now known to range from the Jurassic to the Cenozoic (Tralau 1973). In a study by Tralau (1973), well preserved fossil logs, spores and pollen from a nearby volcaniclastic deposit were studied, and an early to middle Jurassic age was proposed. One-year earlier Printzlau & Larsen (1972) had published the first radiometric datings of the basalts using K/Ar geochronology. Their results indicated a Cretaceous age whereas a couple years later, Klingspor (1976) presented K/Ar dates ranging from the Jurassic to the Cretaceous. In her study, the basalt originally dated as Cretaceous by Printzlau & Larsen (1972), was re-dated as being of Jurassic age. Since then, more radiometric datings have been performed using the more robust 40Ar/39Ar dating technique, resulting in an age span from early Jurassic to early Cretaceous (Bergelin 2009; Bergelin et al. 2010; Tappe et al. 2016), i.e., in the same age range as the K/Ar dates presented by Klingspor (1976). Paleomagnetic measurement are in agreement with an early Jurassic age for several of the outcrops (Bylund & Halvorsen 1993). When the Swedish Geological Survey (SGU) conducted bedrock mapping of the CSVP area in the beginning of the 1990's numerous basalt localities were described, though no additional volcaniclastic deposits were identified (Wikman et al. 1993; Wikman & Sivhed 1993). Although much of the focus has been on the basalts, their origin and absolute ages have been investigated and debated (Tappe 2004; Bergelin 2009; Bergelin et al. 2010; Tappe et al. 2016). The debate have been over the duration of the volcanic activity with Bergelin finding three different pulses (191-176 Ma, 145 Ma & 110 Ma) while Tappe debates only a single pulse around 176 Ma.

In more recent years the volcaniclastic deposits in the CSVP have regained new focus, much because of exceptional preservation of wood and other plant remains, some of which shows different growth stages at a cell-scale (Augustsson 1999; Augustsson 2001; Bomfleur et al. 2014; Bomfleur et al. 2015; McLoughlin & Bomfleur 2016; Vajda et al. 2016).

2 Geological setting

The Mesozoic basalts and volcaniclastic remnants of the CSVP are located in the central parts of Skåne and comprises all the basaltic deposits in Figure 1 and all but three deposits in Figure 2. The CSVP is located near the area where two major tectonic zones intersect; the Proterozoic N-S trending Protogine Zone (PZ) and the NW-SE trending Sorgenfrei-Tornquist Zone (STZ).

The Protogine Zone is a term used since the early days of scientific geology in Sweden, but its tectonic origin, age and extension have been debated for many decades (Andréasson & Rodhe 1990; Wahlgren et al. 1994). In this thesis, the Protogine Zone is recognized as a N-S trending, ca. 25–30 km wide zone of discrete shear zones of both brittle and ductile deformation, stretching from the southern end of lake Vättern and southwards through Småland and Skåne. It disappears under Phanerozoic sedimentary rocks southwest of Romeleåsen horst, southern Skåne (Wik et al. 2006). The zone broadly defines the eastern boundary of the ca. 1.3-0.95 Ga Sveconorwegian orogeny. It has a long and complex tectonic history as indicated by three different generations of mafic and felsic intrusions located along the zone, dated at 1.56, 1.2 and 0.95 Ga (Ask 1996; Jarl 2002; Söderlund et al. 2004; Söderlund & Ask 2006). The youngest event of deformation and metamorphism is connected to the Sveconorwegian orogen that presumably overprints much of the earlier events (Ulmius et al. 2018). Some brittle deformation is probably of younger (post-0.95 Ga) age.

The Tornquist lineament stretches from the North Sea to the Black Sea (Teisseyre 1893; Tornquist 1908; Tornquist 1910; Sorgenfrei & Buch 1964). The northwestern half, known as the Tornquist fan, spreads out between the North German-Polish Caledonian deformation front in the south and the Fennoscandian shield in the north with the most prominent structure represented by the Sorgenfrei-Tornquist zone (STZ) (Sorgenfrei & Buch 1964). The southern boundary of the STZ runs between the Danish island of Bornholm and Skåne. From there it runs through the middle of Skåne in a SE-NW direction and continues to the North Sea through the Kattegat strait and northernmost Denmark (Erlström 2020).

The STZ started to form roughly 290 million years ago, as hundreds if not thousands of diabase dikes intruded the bedrock of Skåne. This is within the same timespan as other events of regional magmatism; the Oslo rift, the British Midland valley swarm, the diabase sills in the table mountains in the province of Västergötland in southern Sweden, and large volcanic deposits in the North Sea and northern Germany (Priem et al. 1968; Michelsen & Nielsen 1993; Ernst & Buchan 1997; Ahlberg et al. 2003; Obst & Katzung 2006; Torsvik et al. 2008; Timmerman et al. 2009; Erlström 2020). The cause of magmatism is not fully understood where one of the two leading theories invokes a mantel plume in the North Sea, just north of the Danish province of Jutland (Ernst & Buchan 1997; Torsvik et al. 2008; Hounslow et al. 2012). The other theory suggests magmatism associated tectonic activity during the aftermath of the Variscan orogeny (Timmerman et al. 2009; Erlström 2020). As the magmatism waned and the stresses in the STZ started to shift during the late Permian, block faulting became dominant. This was not just the case in the STZ but in most of the Tornquist fan which eventually led to the formation of the Danish basin (Erlström 2020). The correlation between the CSVP and the intersection between the Protogine zone and STZ have been di-

scussed since the earliest descriptions of the CSVP until more recently (Nathorst 1887; Wikman & Sivhed 1993). No actual evidence for the connection has however been presented.

The basalt occurs as previously mentioned in over one hundred outcrops and drill sites in the CSVP (Fig. 2). The few times the contacts have been observed it has been through private water well drillings and then between the basalts and the Precambrian crystalline basement (SGU). Bölau (1966) reported contacts between basalt and tuff in several drillings. The volcanic rocks also superimposed sandstones that he palynologically dated to early Jurassic. In one of the drillings the basalt was layered between two tuff layers.

2.1 The Djupadalsmölla volcaniclastic deposit

One of the few and by far best exposed natural section of the volcaniclastic deposits is the classical locality along the Rönne river valley at Djupadalsmölla (Fig. 2). The outcrop is ca 20 m wide, ca 10 m high and today with abundant scree and overgrowth. A few smaller outcrops exist nearby and downstream the main outcrop. At the riverbank, ca 20 m northeast of the main outcrop, granitic basement rock is visible. This suggests a close proximity to the boundary between the old basement rocks and the Jurassic volcaniclastic rocks in this area. According to Wikman et al. (1993) the volcaniclastics rest immediately on top of kaolinitisied basement rock (herein referred to as the sub-Jurassic weathering surface) near the herein studied locality, whereas it rest on sandstone and claystone with some coaly layers only ca 100 m south of this outcrop. Norling et al. (1993) described a complete transition at a small dug out section near the main outcrop at Djupadalsmölla. Their section was composed of a kaolinized basement overlain by two meters of alternating beds of claystone and sandstone with abundant plant fossils. This succession was overlain by a one-meter-thick layer of volcaniclastics with accidental lithics/xenoliths of different origins and plant remains. The volcaniclastics were overlain by 1-2 meters of Quaternary deposits.

A few early studies have been based on this locality (Tullberg & Nathorst 1880; Eichstädt 1883; Svedmark 1883), whereas the only more recent study is by Augustsson (2001). None of these studies focused on describing the stratigraphy of the volca-

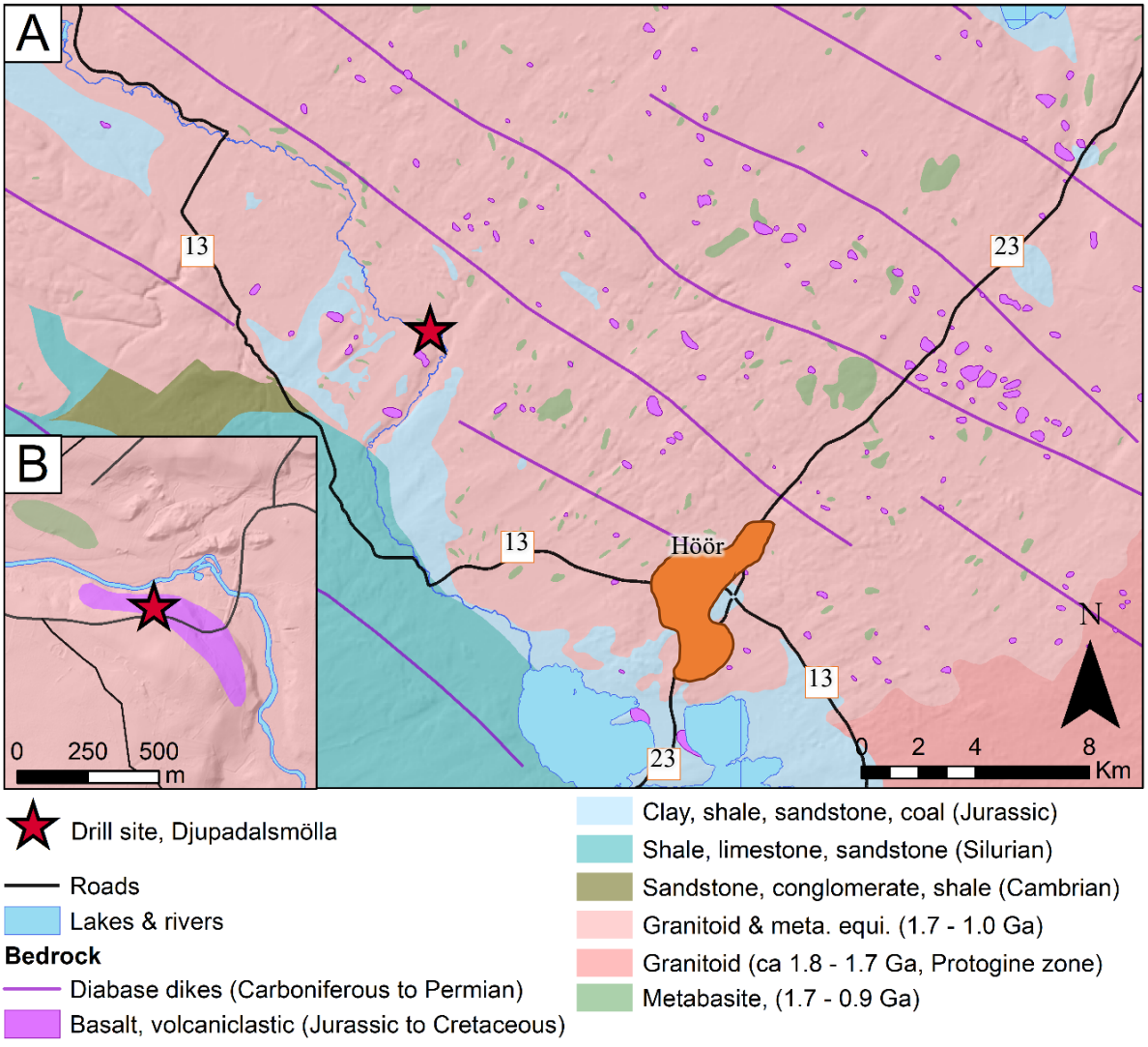

Figure 2. A) Geological map covering most of the Central Skåne Volcanic Province (CSVP). B) The drill site location (red star) and known extent of the volcaniclastic deposit along Rönne river at Djupadalsmölla. Map data: Lantmäteriet© & SGU©.

niclastic succession or its relationship to the weathered basement surface below. Due to the poor quality of the outcrop and a general lack of data, a drilling project was launched by the Department of Geology at Lund University in 2012, and in the summer that year two behind-the-outcrop cores were extracted from just above the main outcrop. The first coring attempt (KBH1) was abandoned early due to problems with drilling in the lose sediments and only ca 10 m of this core was retrieved. The second core (KBH2) reached a total depth of 27,85 m, corresponding to a level ca 8 m below the top of the weathered crystalline basement. Both cores are stored at the Department of Geology, Lund University.

3 Material and methods

The rocks of the KBH2 core are rich in fissures and in many parts poorly consolidated. For this reason, almost 25% of the volcaniclastic succession is preserved only as rubble in the core boxes. The core was split where it was possible and polished (samples D-(1-13)-21-L) to describe the general facies and thin sections were produced for petrographic study. The logging was done in 1:10 scale to not lose the finer details that could be recognized in the core.

Three samples for palynological analysis were collected from a ca 0.3-m-thick mudstone interval between the crystalline basement rocks and the volcaniclastic rocks. Three narrow stratigraphic intervals, each ca 1-2 cm thick, were selected for this sampling (samples D-(I-III)-21-K); their lowest point (tilted) located at 0.01, 0.15 and 0.23 m above the base of the mudstone, respectively. The three samples were prepared at GEUS, Copenhagen, as follows: 20 g of bulk rock was treated in alternating steps with hydrochloric (38%) and hydrofluoric (40%) acid to remove carbonate and silicate mineral phases, according to standard palynological processing described in Poulsen et al. (1990). After washing to neutrality, residues were sieved with 11 μm mesh-size sieves and mounted on strew slides. The samples were analysed by Sofie Lindström and up to 300 palynomorphs were counted per slide with a compound microscope at 650x magnification. A sample collected by Ingemar Bergelin and previously analysed by Sofie Lindström was also included in the data set (D-IV-12-K). Abundance data for every palynomorph taxa were calculated as percentages of the total counted palynomorphs in each of the four samples. Secondly, abundance data for all none reworked spores and pollen were calculated. This could then be recalculated into parent plant abundance by known correlations (Abbink et al. 2004; Petersen & Lindström 2012; Lindström et al. 2017) and thereafter to photic niche distribution as well as plant related environmental distribution.

At the same levels as the three palynomorph samples, D-(I-III)-21-K, were taken from samples were also taken for thin section preparation (sample series D-(I-III)-21-L). The material for these samples were composed of rock fragments that had been glued together and then polished. For this reason, there is no stratigraphic orientation for these samples.

Two sets of thin sections were produced from the core; one at the time of drilling in 2012 (sample series D-(1.1-10.3)-12-E), and one for the current study (sample series D-(2-13, I-IV)-21-E). The original thin sections of the volcaniclastics and the crystalline basement were produced in Erlangen from 10 different samples. In total 9 large and 11 small thin sections were produced. The newer thin sections were also sent to Erlangen for preparation (2021). They were partly from the same sample depths as the original (D-(1.1-5.4, 7.2-10.3)-12-E) but with two additional samples of the volcaniclastic material as well as one from a suspected basaltic clast (D-(11-13)-21-E). Several polished slabs and thin sections were also made from the mudstone underlying the volcaniclastic deposits, after preparation in Erlangen (I-IV).

The original thin sections from the basement and the ones from the mudstone made in Lund were used for mineral/rock classifications and the original volcaniclastic sections were used for point counting for classification and for calculation of total porosity of the rocks. For this, they were first scanned and enhanced using photoshop smart sharpening filter with settings 250% zoom and 2.5 radii. After this the software JMicroVision was used for counting of 300 points per thin section in the volcaniclastic thin sections. Due to the degraded state of the volcaniclastic material the grainsize could only be accurately determined in the thin sections. Thin sections were also examined in polarized light microscope and scanning electron microscope (SEM) to identify changes in chemical and mineralogical composition through elemental mapping using energy dispersive X-ray spectroscopy (EDX).

Table 1. Naming of the sample series with old names to identify them more easily and production year. The naming scheme works as follows. The first letter in the code is for Djupadalsmölla. The following number (roman numbers as well) is the sample number of that specific series. The second number (12 or 21) is the production year. Last letter stands for the city where it was produced in (E-Erlangen, K-Copenhagen, L-Lund).

Sample series	**Old name**	**Production year**
D-(1.1-10.3)-12-E	"original" 1.1-10.3	2012
D-(IV)-12-K	Old palynology sample	2012
D-(I-III)-21-L	Thin sections I-III	2021
D-(2-8, 9-9.2, 10-11, 11o, 12-12.3, 13, I-IV)-21-E	"new" 2-8, 9-9.2, 10-11, 11o, 12-12.3, 13, I-IV	2021
D-(I-III)-21-K	Palynology sample I-III	2021
D-(1-13)-21-L	Polished slab 1-13	2021

4 Results

The core section includes three distinct rock units, in ascending order; 1) Crystalline basement that is deeply kaolinite weathered (6.32 m), 2) A dark-grey mudstone unit rich in palynomorphs (0.3 m), and 3) Greenish grey to blackish volcaniclastic rocks (19.5 m). The reference level used herein corresponds to the boundary between the weathered crystalline basement and the overlying mudstone and is situated 20.50 m below ground surface (Fig. 3). Below follows a description of the three rock units.

4.1 The crystalline basement

The crystalline basement rock is a reddish to whitish gneiss and encompass the lowermost 6.32 m of the core. The gneiss is invariably weathered and altered. The lowermost cored meter (-6.32 to -5.35) differs from the rest of the unit in being dominated by mafic minerals that form ca 0.5 m thick mafic band (Fig. 4A). Similar mafic bands are relatively common in outcropping
gneiss further north of the locality. Within this mafic band there are several small veins of coarse-grained quartz and k-feldspar. The upper 5.35 m of the basement is devoid of more pronounced mafic bands. The gneissic fabric becomes less distinct towards the top due to an increasing degree of weathering. Pink feldspars are visible from the base of the core until -3.50 m below the reference level. Two levels with larger quartz crystals occur at -3.60 and –0.25 m. At ca -4.00 m the gneiss is weathered extensively to a cream white kaolinite clay. At the top, -0.30–0.00 m, the gneiss is weathered to a similar white kaolinite clay with sparse quartz grains. Comparison of driller's notes on the core boxes and own measurement of the core suggests that ca 1.20 m of the top of the core was lost during drilling, likely because of the soft character of the weathered material in this part of the core. This means that the nature of the original contact to the overlaying mudstone is unknown.

In the two thin sections produced from the crystalline basement an upward increase in the degree of weathering was evident. In sample D-1.1-12-E quartz and k-feldspars were identified as well as unidentified oxides (Fig. 5A). There are abundant degraded mafic minerals as well, that could not be identified. No plagioclase was detected in this sample. In sample D-2.1-12 -E quartz is the only mineral that could be identified with all other minerals heavily altered (Fig. 5B). The altered minerals create an amorphous matrix in between the quartz grains with some darker spots assumed to represent degraded, mafic minerals.

4.2 The Mudstone unit

The mudstone unit varies from light greyish to dark greyish in colour and consists of ca 0.30 m of silt and clay in different ratios and poorly defined layers (Fig. 6). The bedding planes are tilted 20-30° from the horizontal plane. In the darker coloured sections, at ca +0.01 and +0.15 m, small flakes of coaly material occur. Small-scale and poorly preserved bedforms, most likely ripples, with a maximum amplitude of ca 1 cm, can be seen through most of the unit. Several micro-faults occur in the lower sandy section of the mudstone (Figs. 7-8). Towards the top, the mudstone is successively displaced by the volcaniclastics and at the top of the unit, a few larger volcaniclastic fragments are embedded in the mudstone.

A first set of thin sections (D-(I-III)-21-L) from the mudstone were produced from material of the core without known orientation relative to the core. These samples were taken at the same levels as the samples for palynology and are described below.

Sample D-I-21-L consist of coarse silt - fine sand grains (0.2-0.02 mm) in a matrix of clay (Fig. 9A). Some larger grains reach into the lower range of medium sand. The grains consist mostly of quartz with subordinate small black fragments (<0.5 mm). The latter fragments are angular and in most cases one axis is longer than the other two.

Sample D-II-21-L is more fine-grained than sample I, with no quartz grains being larger than 0.02 mm (coarse silt; Fig. 9B). In this sample the black fragments were more numerous and also larger, although rarely over 0.05 mm, than in the previous sample, but still only makes up a very small part of the rock.

Sample D-III-21-L is made up of silt sized grains (<0.02 mm) in a clay matrix (Fig. 9C) and with subordinate larger quartz and k-feldspar grains in the 0.05-1 mm size range. Some areas of the sediment around these larger grains contain higher levels of sulphur (Fig. 10). Unlike previous samples, no black fragments were seen.

4.3 Palynomorphs from the mudstone unit

In the four samples a total of 100 different taxa, were identified. Of these 80 were pollen and spores (land plants) and 9 were identified as reworked material of an older age (Fig. 11-12, Table 2). The rest of the palynomorphs constitutes dinoflagellate cysts, acritarchs and algae (Fig. 12-13). Three palynomorphs, *Callialasporites turbatus*, *Mancodinium semitabulatum* and a putative *Nannoceratopsis gracilis* (Fig. 13G), have their first appearance datum (FAD) in late Pliensbachian (ca 185 Ma) whereas the reminder has a much broader temporal distribution (Poulsen & Riding 2003). Both dinoflagellate cysts indicative of marine influences and algae, especially the microalga Botryococcus indicative of lacustrine to brackish environment were noted (Fig. 13; (Guy-Ohlson 1998).

The aquatic palynomorphs makes up 5-9% of the total palynomorph count (tpc; Fig. 12). Of these the different dinoflagellate cysts dominate with 3-8% tpc while the other aquatic palynomorphs all together never reach over 2% tpc. Palynomorphs that couldn't be identified constituted 0-13% tpc while spores and pollen (land plants) account for 82-94% tcp (Figs. 11-14).

The dominant palynomorph in all four samples, *Perinopollenites elatoides* (Figs. 11-15c), accounting for 24-36% of total none reworked sporopollen count (tnrsc), were coming from *Taxodium* (a kind of swamp cypresses; Abbink et al. 2004; Lindström et al. 2017). As the name implies these trees preferred to grow in very wet environments like swamps and mires making up much of the upper canopy (Table 2, Fig. 14). Two other palynomorphs that were common, *Deltoidospora toralis* (Fig. 16b) and *Deltoidospora minor* (Fig. 16d) were derived from ferns in the groups *Dipteridaceae* and *Dicksoniaceae* (Fig. 11). They made up the under-

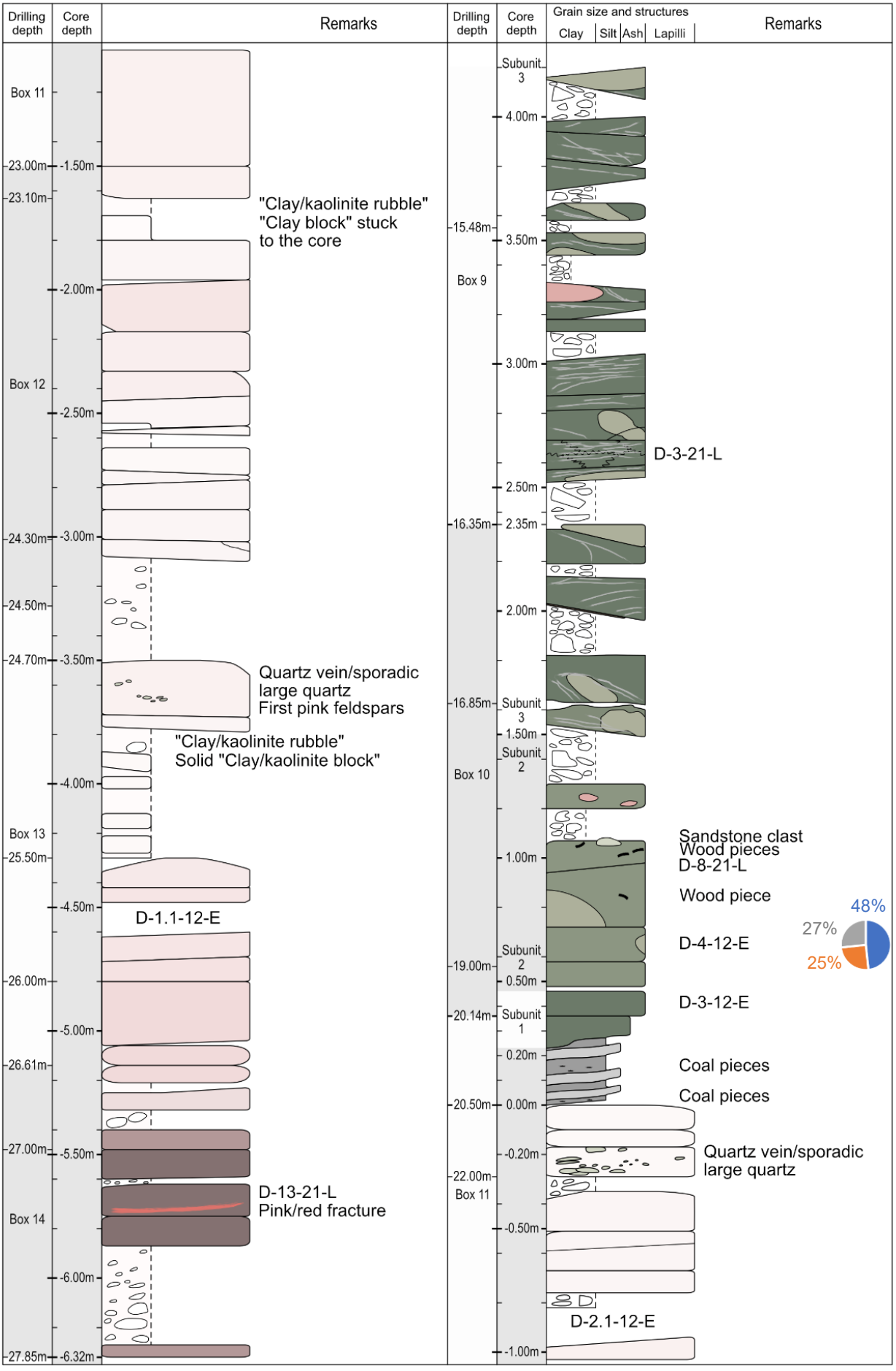
Drilling depth
Core depth
Remarks
Box 11
23.00m
-1.50m
23.10m
"Clay/kaolinite rubble"
"Clay block" stuck
to the core
-2.00m
Box 12
-2.50m
24.30m
-3.00m
24.50m
24.70m
-3.50m
Quartz vein/sporadic
large quartz
First pink feldspars
"Clay/kaolinite rubble"
Solid "Clay/kaolinite block"
-4.00m
Box 13
25.50m
-4.50m
D-1.1-12-E
26.00m
-5.00m
26.61m
27.00m
-5.50m
D-13-21-L
Pink/red fracture
Box 14
-6.00m
27.85m
-6.32m
Drilling depth
Core depth
Grain size and structures
Clay
Silt
Ash
Lapilli
Remarks
Subunit 3
4.00m
15.48m
3.50m
Box 9
3.00m
D-3-21-L
2.50m
16.35m
2.35m
2.00m
16.85m
Subunit 3
1.50m
Subunit 2
Box 10
Sandstone clast
Wood pieces
D-8-21-L
1.00m
Wood piece
48%
27%
25%
D-4-12-E
Subunit 2
19.00m
0.50m
D-3-12-E
20.14m
Subunit 1
0.20m
Coal pieces
Coal pieces
20.50m
0.00m
-0.20m
Quartz vein/sporadic
large quartz
22.00m
Box 11
-0.50m
D-2.1-12-E
-1.00m

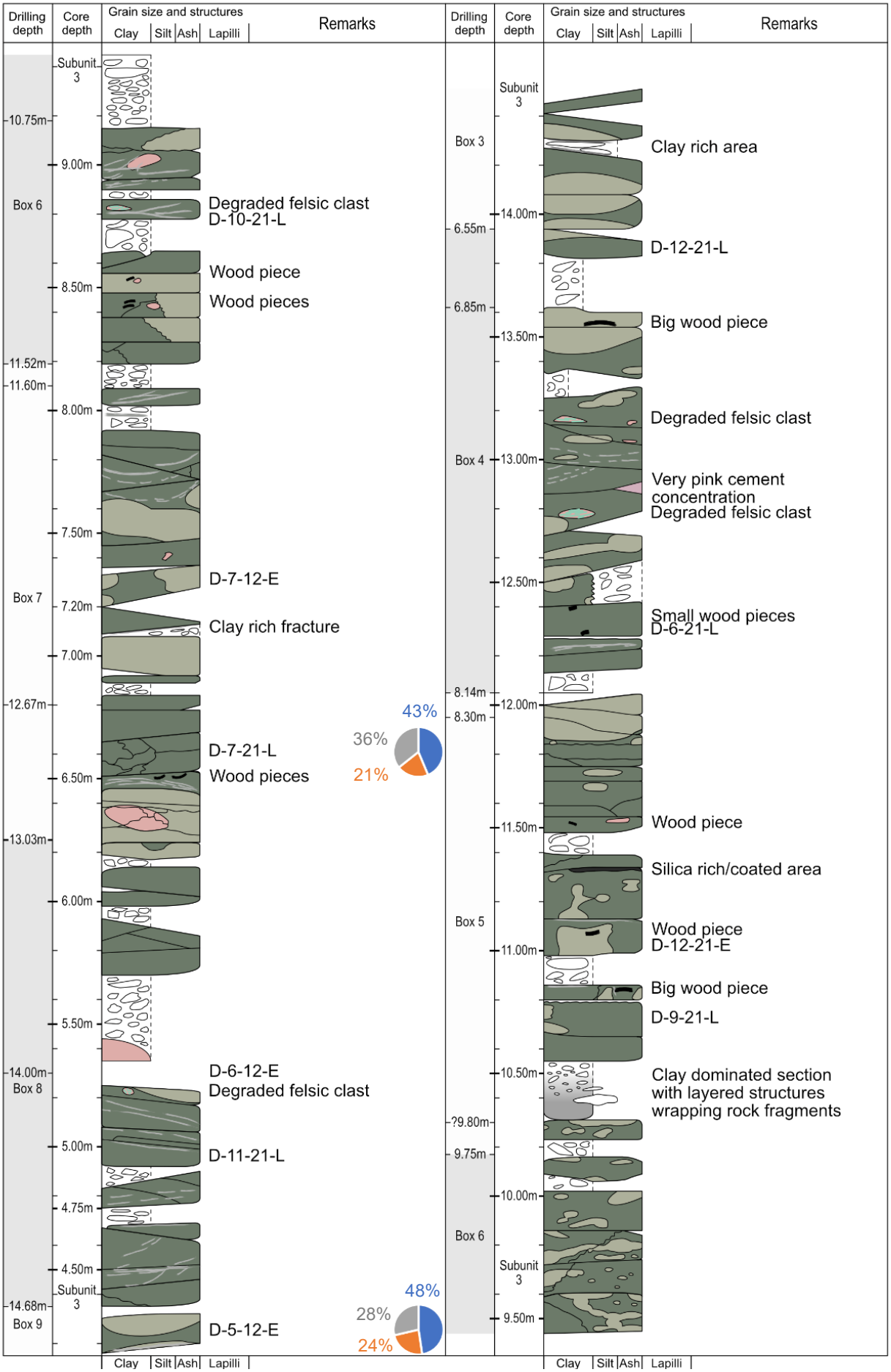
Drilling depth
Core depth
Grain size and structures
Clay
Silt
Ash
Lapilli
Remarks
Subunit 3
10.75m
9.00m
Box 6
Degraded felsic clast
D-10-21-L
Wood piece
8.50m
Wood pieces
11.52m
11.60m
8.00m
7.50m
D-7-12-E
Box 7
7.20m
Clay rich fracture
7.00m
12.67m
43%
36%
21%
D-7-21-L
6.50m
Wood pieces
13.03m
6.00m
5.50m
14.00m
Box 8
D-6-12-E
Degraded felsic clast
5.00m
D-11-21-L
4.75m
4.50m
Subunit 3
14.68m
Box 9
48%
28%
24%
D-5-12-E
Box 3
6.55m
6.85m
Box 4
8.14m
8.30m
Box 5
?9.80m
9.75m
Box 6
9.50m
14.00m
13.50m
13.00m
12.50m
12.00m
11.50m
11.00m
10.50m
10.00m
Clay rich area
D-12-21-L
Big wood piece
Degraded felsic clast
Very pink cement concentration
Degraded felsic clast
Small wood pieces
D-6-21-L
Wood piece
Silica rich/coated area
Wood piece
D-12-21-E
Big wood piece
D-9-21-L
Clay dominated section with layered structures wrapping rock fragments

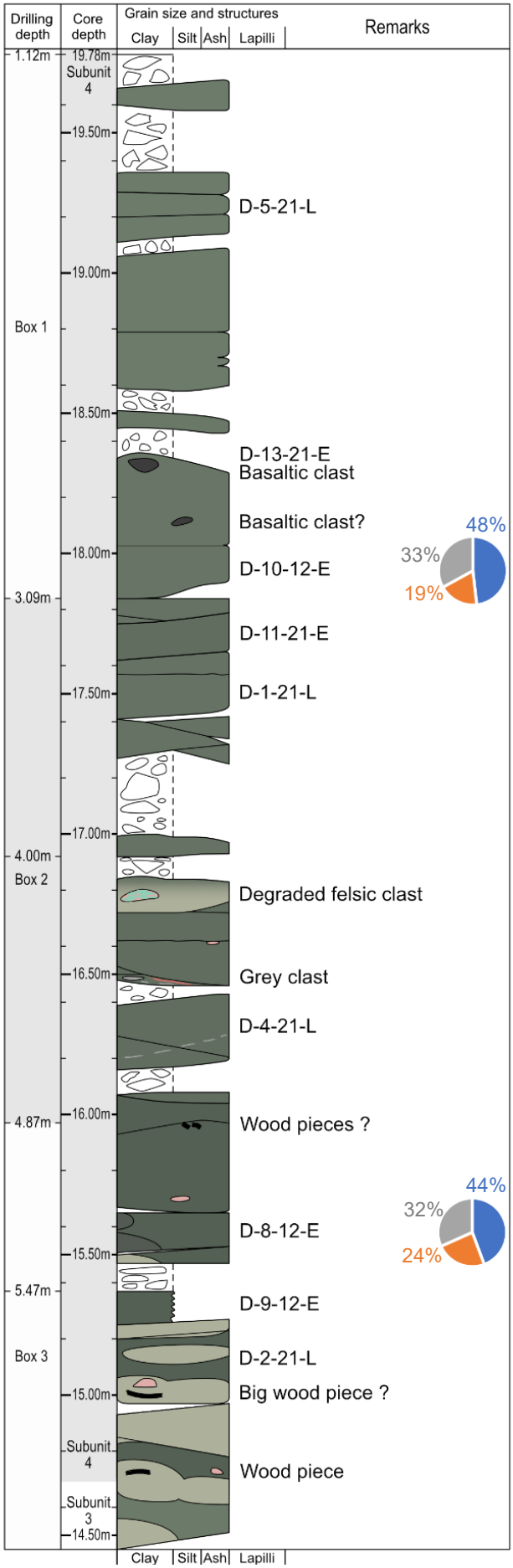
Drilling depth
Core depth
Grain size and structures
Clay
Silt
Ash
Lapilli
Remarks
1.12m
19.78m
Subunit 4
19.50m
D-5-21-L
19.00m
Box 1
18.50m
D-13-21-E
Basaltic clast
Basaltic clast?
48%
33%
19%
18.00m
D-10-12-E
3.09m
D-11-21-E
17.50m
D-1-21-L
17.00m
4.00m
Box 2
Degraded felsic clast
Grey clast
16.50m
D-4-21-L
4.87m
16.00m
Wood pieces ?
44%
32%
24%
D-8-12-E
15.50m
5.47m
D-9-12-E
Box 3
D-2-21-L
15.00m
Big wood piece ?
Subunit 4
Wood piece
Subunit 3
14.50m
Clay
Silt
Ash
Lapilli

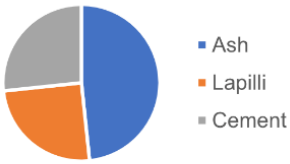
Ash
Lapilli
Cement

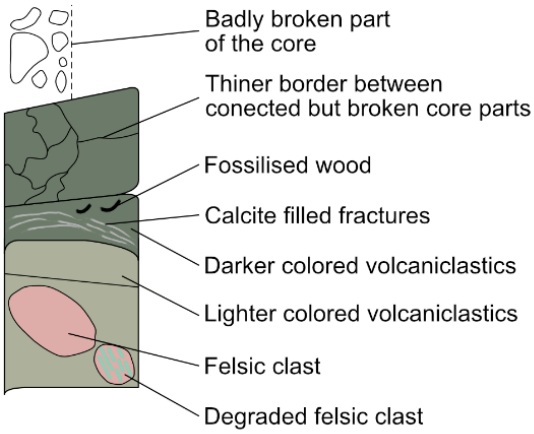
Badly broken part of the core
Thiner border between conected but broken core parts
Fossilised wood
Calcite filled fractures
Darker colored volcaniclastics
Lighter colored volcaniclastics
Felsic clast
Degraded felsic clast

Figure 3. Sedimentary log profile of the Volcaniclastic deposits of the KBH2 drill core from Djupadalsmölla. The log is made in scale 1:10 with the first column representing the depth noted during drilling and here is also noted what core box the certain section is stored in. The second column represent the logging depth based on the contact between the weathered basement and the dark-coloured mudstone as reference level. Here the volcaniclastic subunits are marked as well. The relative difference between the measurements in the first and second column can be seen as the degree of core loss or expansion due to fragmentation. Three main rock units can be separated in the core. The lowermost unit is the weathered crystalline basement that was cored to a depth of 6.32 m below the basement surface. It includes a thicker mafic band in the lowermost part succeeded by several levels of highly weathered gneiss. The k-feldspars show an increasingly degraded state and whitening towards the top of the basement. At the top, the gneiss has degraded fully to kaolinite clay with quartz grains. The basement is overlain by a ca 0.3-m-thick, dark-coloured mudstone unit including a rich and diverse palynomorph fauna and tiny coal/vitrinite fragments. The third and uppermost rock unit encompass the volcaniclastic strata subdivided in four subunits. The subunits do not represent major petrographic differences but more likely reflect post-depositional diagenetic changes and should therefor only be used to navigate in the core. Subunit 1 is only 0.23 m thick and is characterised by a low degree of preserved volcaniclastic texture and a high degree of core loss. The second subunit is 1.02 m thick and characterised by a well-preserved volcaniclastic texture, light coloured pseudo-nodules, and several wood fragments. The third subunit is the longest, stretching from +1.50 to +14.75 m. Due to the much larger size of this subunit there are more changes, but the most characteristic ones are the poorly consolidated state of the material, the many cement filled fractures and a shift from light (in subunit 2) to dark pseudo-nodules. The uppermost subunit (4) is 5.03 m thick and is characterised by its darker colour and well consolidated state. The pie charts to the right of the log show point counting results. Note the even proportion of ash around 45% in all samples. The proportion of intergranular cement shifts the most between sample D-4.3-12-E at 27% and D-7.2-12-E at 36%.

story in the forests they lived in and were common in drier patches in mire like environments. *Alisporites robustus* is another common palynomorph coming from a seed fern from the group *Corystospermales* that lived in waterlogged conditions in mire like environments and made up the upper canopy just like Perinopollenites. Lastly, *Pinuspollenites minimus* (Fig. 15f) coming from pinacean coniferes living in dryer areas appear towards the top of the mudstone. Worth noting is the low amounts of *Classopollis* (Figs. 11-15a) in all the samples. *Classopollis* was produced by a family of conifers, the *Cheriolepideaceae*, and some of its members could tolerate dry and/or saline environments and may have preferred to live like today's mangrove trees (Abbink et al. 2004).

When it comes to the composition of the vegetation most of the pollen came from gymnosperms (53-61% of tnrsc) and secondly ferns (30-39% of tnrsc) with Sphenophytes, Bryophytes and Lycophytes only making up 1-3% of tnrsc (Fig. 11). Within the gymnosperms, conifers dominated, while cycads/ginkgos and seed ferns were common.

For the ferns it was the *Dipteridaceae*/ *Dicksoniaceae* that dominated. In the photic niche, plants making up the canopy is the most common and constitutes 60-69% of tnrsc (Fig. 14). Twenty-three different species from 13 different genera were identified in this photic niche. The understory constitutes 17 -32% of tnrsc, from 3 species in a single genus. Plants creating the ground cover corresponds to 8-15% of tnrsc and 26 species from 24 different genera could be identified. Spores and pollen that are not known from which plants or photic niche they belong to, make up 0 -1% of tnrsc.

When applying the environmental preferences of pollen-related plants, three different articles were used (cf. Fig. 14). The first being Abbink et al. (2004) and the second and third being Petersen & Lindström (2012) and Lindström et al. (2017). The last two were combined since they used the same categories. Abbink et al. (2004) uses different names for some of the environmental categories but are interpreted to be semi-interchangeable with the ones from Petersen & Lindström (2012) and Lindström et al. (2017). This concerns the lowland and upland categories from Abbink et al. (2004) and are interpreted to be corresponding to the mire and well drained categories in Petersen & Lindström (2012) and Lindström et al. (2017). It is also good to note that Petersen & Lindström (2012) and Lindström et al. (2017) has subgroups in these categories that the first set has as its completely own categories. there are some variations seen in the two different interpretations as can be seen in Figure 14. The general consensus in both, is however a wetland area with only a few dryer parts.

4.4 The stratigraphy and sedimentology of the volcaniclastic unit

The volcaniclastic unit is 19.50 m thick and mainly composed of lapilli tuff cemented by calcite or zeolite. Xenoliths (rock fragments picked up before leaving the vent and identified by angularity) and accidental lithics (non-volcaniclastic rock fragments picked up after leaving the vent, identified by higher degree of roundness) are common. They range in size from a couple of millimetres to ca 0.1-0.2 m with the majority having a felsic composition. The volcaniclastic succession shows no obvious bedding features or sedimentary structures and overall appears massive from clay weathering. A striking feature, however, is numerous rounded to sub-rounded bodies of better preserved and more lithified rock that due to their better preservation and colour contrast stands out in the core as pseudo-nodules. These are frequent in most part of the core and facilitate description of the microscopic properties and classification of the rocks (Fig. 17). Although the colour of the pseudo-nodules may vary, petrographic study show that they have a similar composition as the surrounding rock mass. Due to the lack of descriptive sedimentary features a subdivision of the rocks was made based on the colour and contrast of the core. The subdivision includes four parts, herein referred to as volcaniclastic subunits 1-4 (Fig. 3) and these are described below.

Subunit 1 (+0.25-+0.48 m) starts at the transition between the dark coloured mudstone and the volcaniclastics. In the lowermost part of the unit larger lapilli sized clasts are embedded in a fine-grained matrix

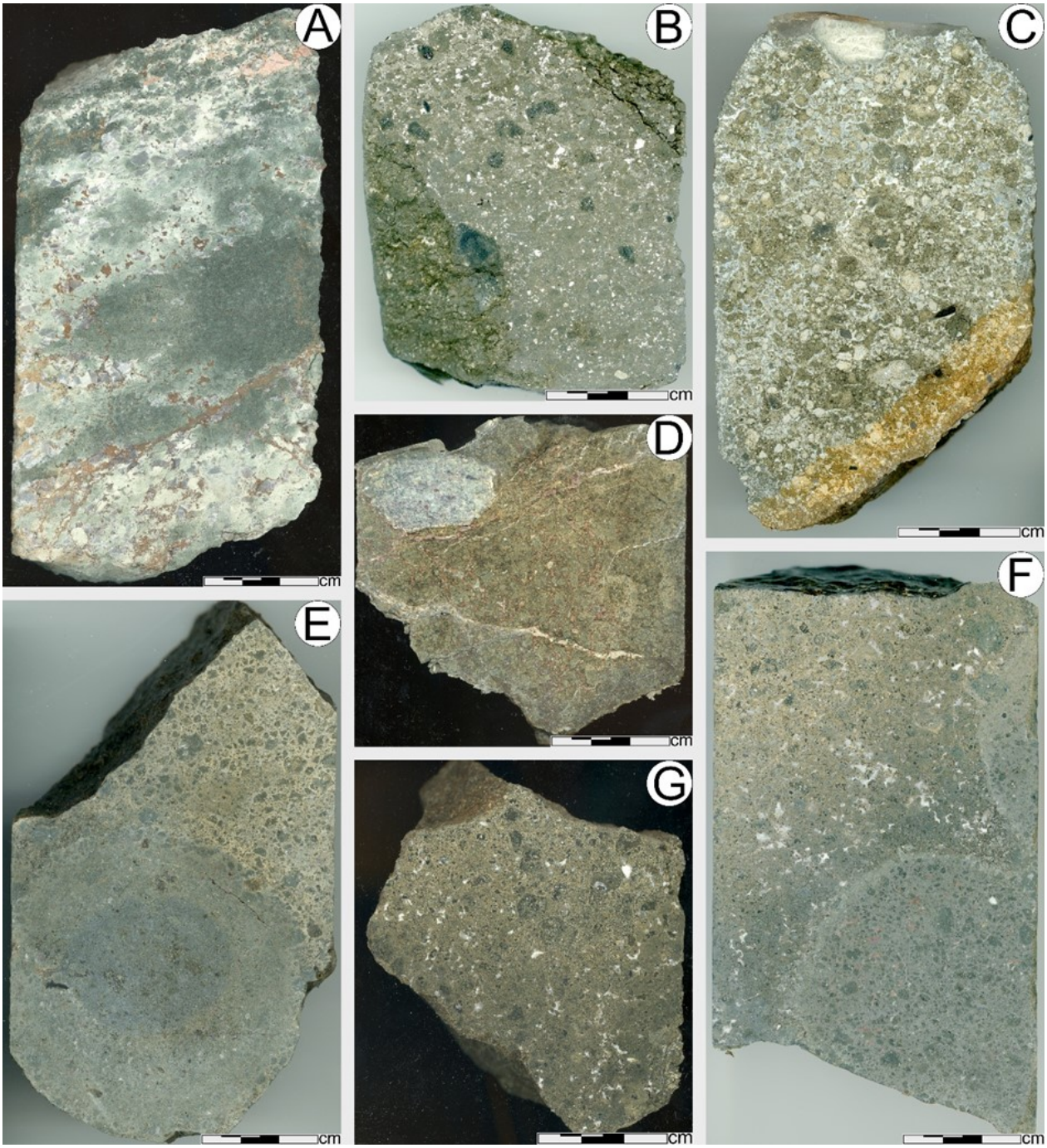

Figure 4. Selected polished slabs from the Djupadalsmölla KBH2 drill core. A) D-13-21-L, -5.70 m. Degraded mafic band in the lowermost part of the core. B) D-3-12-E, subunit 1, +0.40 m. Degraded volcaniclastics from the lowermost part of subunit 1. C) D-8-21-L, subunit 2, +1.00 m. Bright lapilli-tuff with small wood pieces and a sandstone clast at the top. D) D-10-21-L, subunit 3, +9.20 m. Fine-grained lapilli-tuff with a degraded felsic accidental lithic. E) D-12-21-L, subunit 3, +13.90 m. Dark-coloured pseudo-nodule in light-coloured lapilli-tuff. Note that lapilli grains seemingly are absent in the pseudo-nodule, but microscopy reveals that they are present also here although preserved with the same colour. F) D-8-12-E, subunit 4, +15.60 m. Small pseudo -nodules with greenish lapilli grains enclosed in lapilli tuff with abundant cement (light coloured). G) D-5-21-L, subunit 4, +19.25 m. Intermediate dark lapilli tuff from the top of the core.

of unknown composition whereas the upper part of the subunit is more degraded and only occasional larger grains are preserved (Fig. 4B). This subunit is the most degraded part of the core and all other parts of the core show clearer grain boundaries. Important to note is the fact that the top 0.10 m of this subunit (half of the subunit) and lowermost 0.10 m of the next subunit represents an interval with substantial loss of core, ca 80%, which may lead to anomalous facies shifts in the succession.

Subunit 2 (+0.48-+1.50 m) is a lapilli-tuff and starts, as the preservation of the volcaniclastic grains are better, with high contrast between grains and matrix, giving the perception that it is lapilli domina-ted (Fig. 4C). This is not the case as is evident from point counting results (presented further down). A

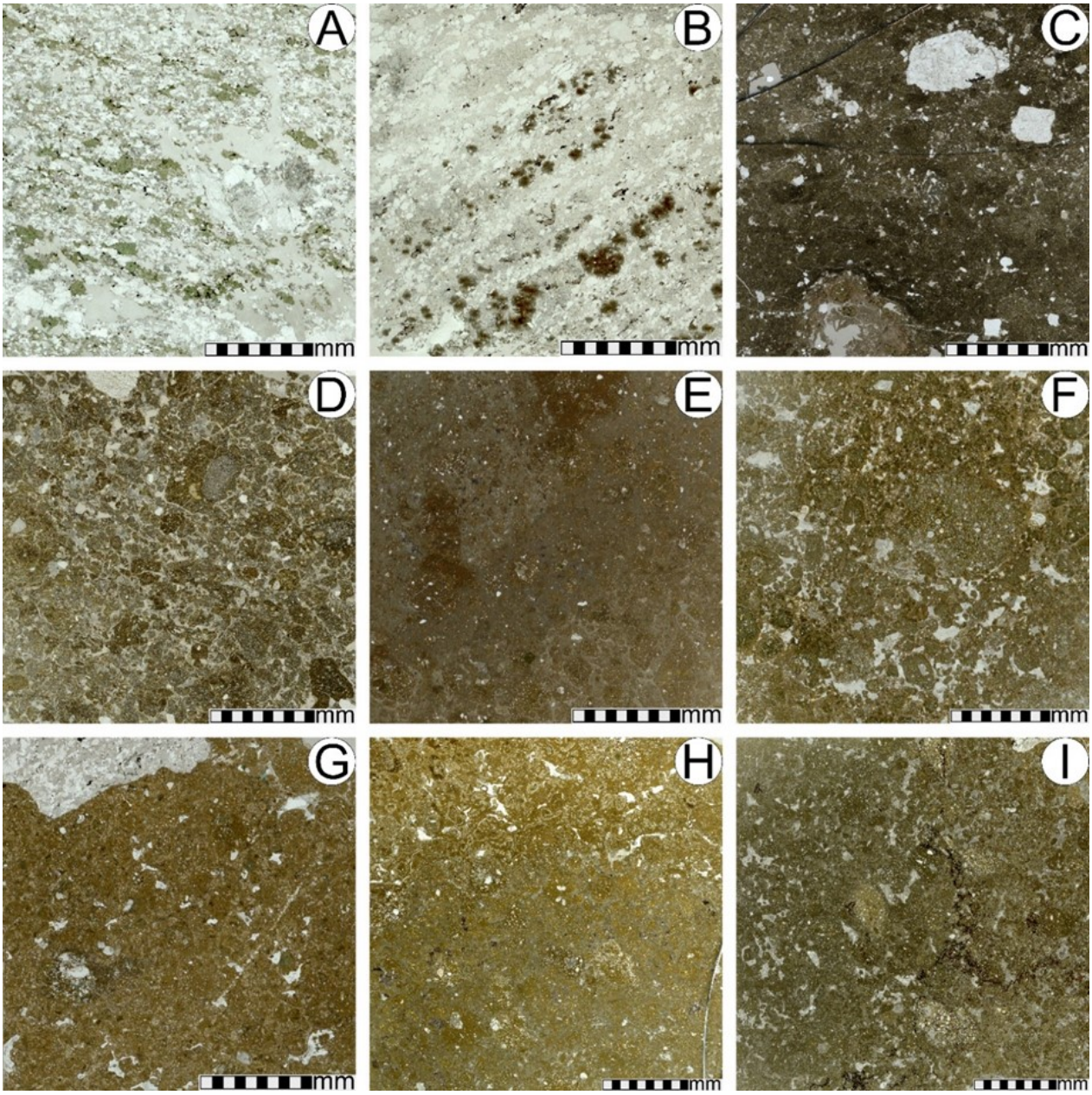

Figure 5. Descriptive photographs of the thin sections. A) D-1.1-12-E, ca -4.50 m. Degraded gneiss with K-feldspars and quartz still intact while other minerals have degraded. B) D-2.1-12-E, ca -0.90 m. Heavily degraded gneiss with only quartz still intact. C) D-3.2-12-E, subunit 1, ca +0.40 m. Heavily degraded volcaniclastic deposit with no clear texture preserved except for two non-volcanic grains. The volcanic glass is replaced by swelling clay minerals (s.c.m.). D) D-4.3-12-E, subunit 2, ca +0.60 m. Degraded lapilli tuff with a clear volcaniclastic texture of angular to subrounded grains replaced with s.c.m. and cemented with calcite or in smaller areas kaolinite. E) D-5.4-12-E, subunit 3, ca +4.20 m. Degraded lapilli tuff with a volcaniclastic texture of angular to subrounded grains replaced with s.c.m. and cemented with Fe rich calcite. F) D-7.2-12-E, subunit 3, ca +7.30 m. Degraded lapilli tuff with a volcaniclastic texture of angular to subrounded grains replaced with s.c.m. and cemented mainly with calcite but both chlorite and zeolite occur as well. G) D-9.1-12-E, subunit 4, ca +15.30 m. Degraded lapilli tuff with a volcaniclastic texture of angular to subrounded grains replaced with s.c.m. and cemented mainly with calcite but both chlorite and zeolite are common as well. H) D-8.2-12-E, subunit 4, ca +15.60 m. Degraded lapilli tuff with a volcaniclastic texture of angular to subrounded grains replaced with s.c.m. and in the lower two thirds cemented with Fe rich calcite or in some dark red to brown areas, Ca rich siderite. In the upper one third it is instead zeolite cemented. I) D-10.3-12-E, subunit 4, ca +18.00 m. Degraded lapilli tuff with a volcaniclastic texture of angular to subrounded grains replaced with s.c.m. and cemented mainly with calcite but both chlorite and zeolite occur as well, just as some dark red to brown areas of Ca rich siderite.

clear white cement fills the intergranular porosity and the vesicles. At +0.8 m there is a large pseudo-nodule with intense white cement and almost black grains, a feature that is characteristic for the pseudo-nodules in this subunit. Near the same level (+0.8 m) is the first piece of petrified/charred wood. In the polished slab centred around 1.00 m (Fig. 4E), three small fragments of charred wood were noted, which are a couple of mm in size. At the top of the polished slab there is an accidental lithic fragment of sandstone, 30 x 20 x 10

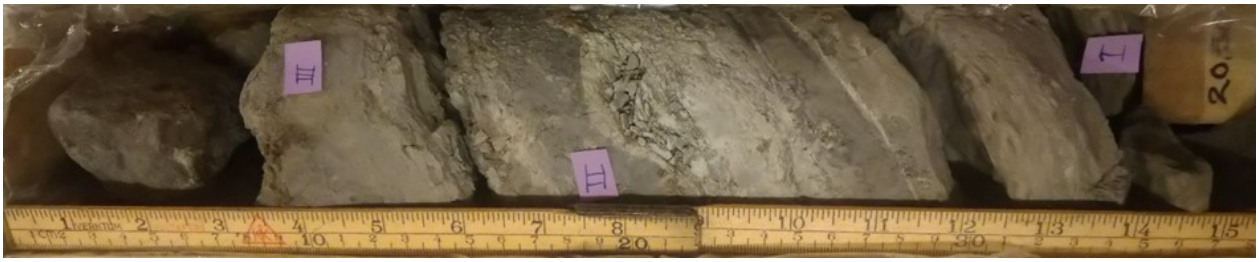

Figure 6. The dark-coloured mudstone at the top of the crystalline basement with ca 10-15 cm of volcaniclastics at the top (left). Purple notes indicate locations for samples I-III for palynology and thin sections. Left is up core.

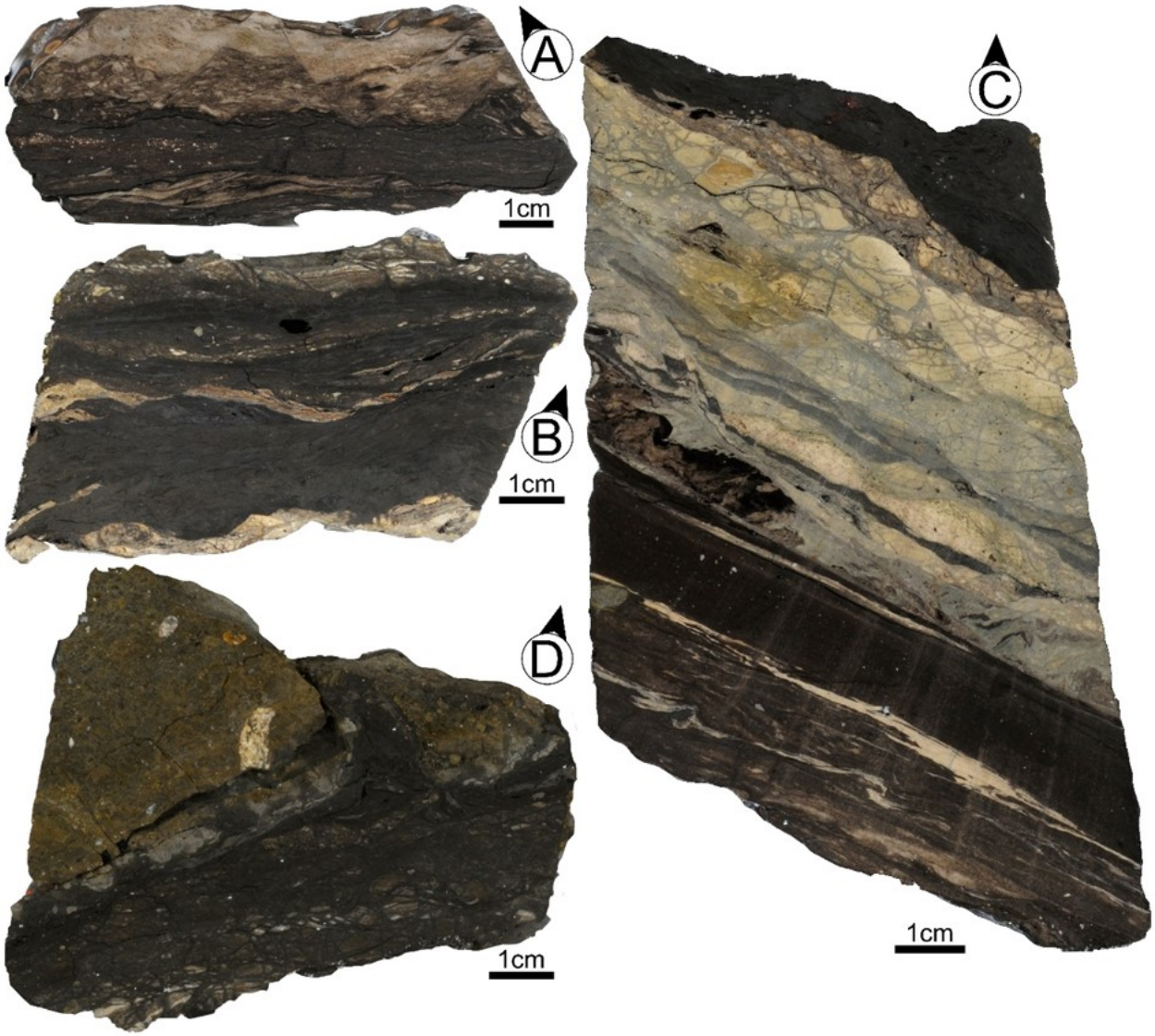

Figure 7. Polished slabs of the dark-coloured mudstone interval. A represents the lowermost portion of the mudstone and D the topmost. Arrow at the latter show the up direction for that part. The mudstone has a shifting lithology from an organic rich clay to a clean quartz arenite. Sedimentary structures can be seen in all parts of the mudstone. Micro-faults can be seen in the sandstone section of A and a close-up of this slab can be seen in Figure 8. In the top of D two larger volcanic clasts are embedded in the mudstone.

mm in size. It is a mineralogically mature and well cemented sandstone with angular grains. This was the only sandstone clast to be identified in the core and it is classified as an accidental clast due to its rounded shape. At +1.25 m, the first two fragments of gneiss or granite were noted. The interval between +0.65 and +1.60 m has a similar composition and appearance as the section below but is affected by core loss as this one meter of material comes from a span of 2.15 m, that is 47% core loss.

Subunit 3 (+1.50-+14.75 m) is a lapilli-tuff that starts as the colour change from the light and grainy texture in subunit 2 to a much darker and lower contrast texture with many small (< 0.2 m) lighter coloured pseudo-nodules in subunit 3 (Fig. 4C-D). The cement/matrix in the subunit is dark with the grains

Fig. 8. Close-up of the lowermost portion of the mudstone (Fig. 7A). In the sandy layer several micro-faults can be seen with the assumed direction of displacement marked with arrows. Note that the section is not correctly oriented and that up in the section is the direction of the black arrow.

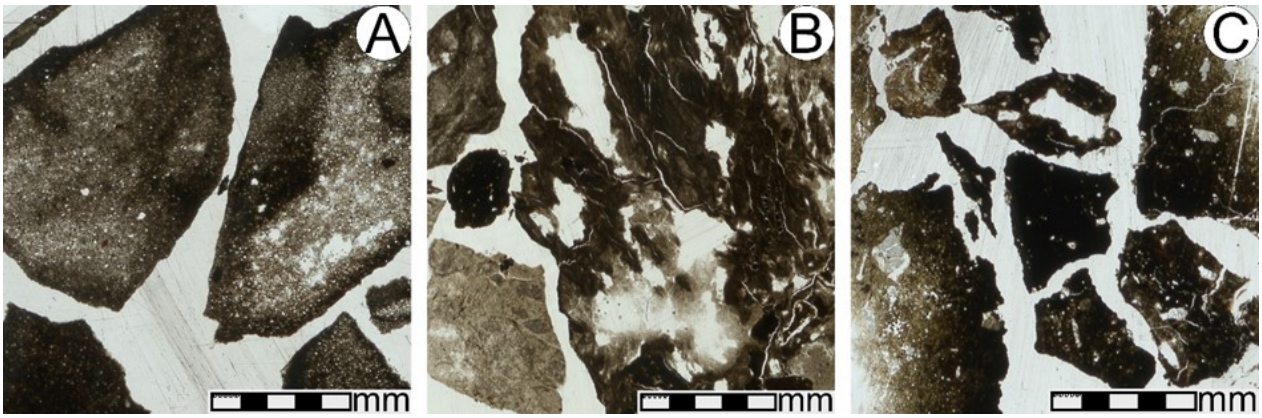

Figure 9. Thin section samples from the three sample levels in the dark-colured mudstone unit. A) Mudrock mainly composed of coarse silt and small coal fragments with subordinate fine sand (D-I-21-L from ca +0.01 m). B) Fine-grained mudrock with the largest fraction being the coaly fragments and quartz in the silt fraction (D-II-21-L, from ca +0.15 m). C) Mudrock with roughly the same grain size as in A but lacking coaly material. Instead, millimetre sized crystals of quartz and K-feldspar are scattered within the sample (D-III-21-L, from ca +0.23 m).

being lighter coloured. The opposite is true for the pseudo-nodules, with lighter coloured cement and darker grains. In a polished slab from +13.90 m, a seemingly oppositely coloured pseudo-nodule, for this subunit, can be seen cut in the middle with some of the surroundings (Fig. 4E). In this pseudo-nodule the contrast between grains and cement are low but it still the same cement to grain ratio as outside of it. Similar observations were also seen in other polished slabs.

In the lower part of subunit 3, white cement-filled fractures have their first occurrence, cutting through the core at low to medium angles (15-50°) from the horizontal plane (Fig. 4D). These closed fractures are more and less abundant throughout subunit 3 and are most common in the interval +1.50 to +5.20 m. The last occurrence of such fracture occurs at +15.20 m, representing the only fracture in subunit 4. At +11.35 m, in an area between two none fractured parts of the core, silica has impregnated the rock. This is the only part of the core where any suspected silicious fluid effects were noted.

At +10.85 a piece of wood measuring 20 x 5 x 20 mm is preserved. Due to the fragmented state of the core at this level it is possible to see the three-dimensional structure of the wood as well as fibrous structures within it (Fig. 18). Four smaller wood pieces occur at +11.10, +11.50, +12.30 and at +12.40 m. At +13.55 the biggest piece of wood of the entire succession was observed, 30 x 6 mm. At +14.70 and +15.00 m another two potential wood pieces being 18 x 3 mm and 23 x 2 mm respectively occurs. The last two wood pieces are uncertain, and both occurs at +15.95 m.

Subunit 4 starts at +14.75 m, where the rock colour changes to almost black for the first two meters. Above this there is a gradual change to a more intermediate grey in the top two meters. The degree of core loss is relatively small and the rocks in this part are better lithified. Less than one meter above the base of the subunit, lighter pseudo-nodules similar to those of the underlying subunits decrease in number (Fig. 4F). There are however similar pseudo-nodules also higher up, although much less distinct (Fig. 4G).

Three accidental clasts and/or xenoliths occur in Subunit 4. The lowermost is dark grey with no obvious internal structure and most likely a sedimentary rock. The second is interpreted to be a basalt although its small size and degraded state make this interpretation uncertain. The third, being larger, was confirmed to be

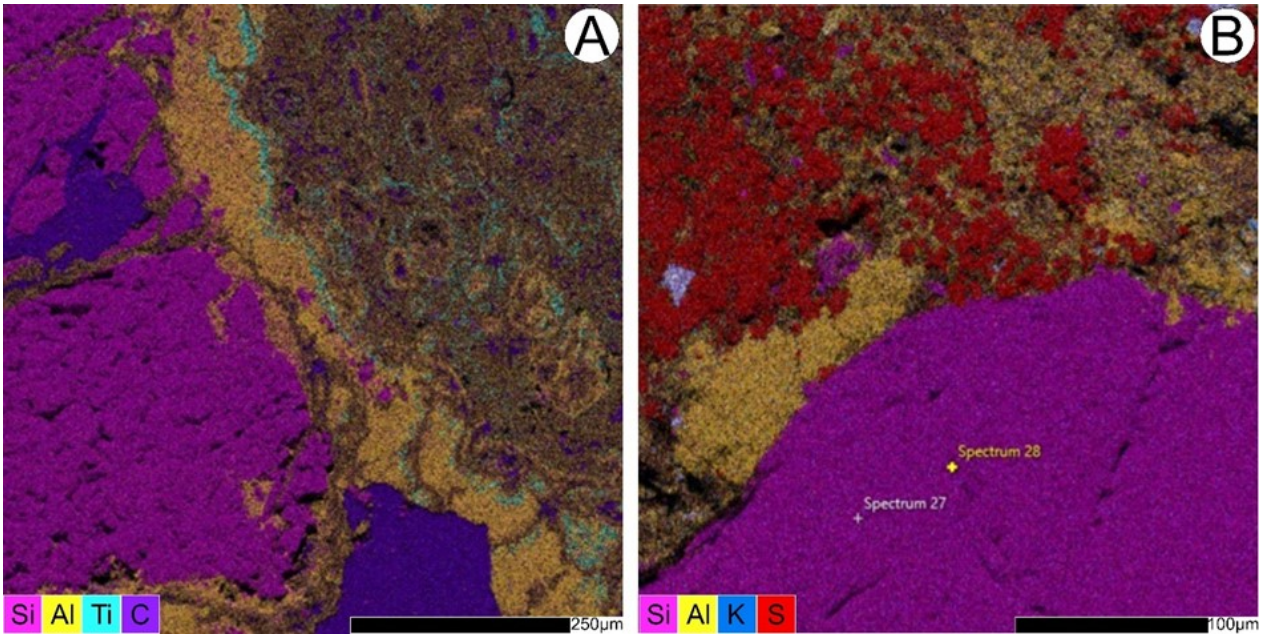

Figure 10. SEM EDX photograph of thin section D-III-21-L from the upper part of the dark-coloured mudstone unit (Fig. 9). The high carbon areas in A are most likely carbon coated glue. In both A and B large quartz grains can be seen and in B a small k-feldspar is visible in the sulphur rich matrix.

a basalt xenolith. It was more angular than most of the other lithics in the core suggesting it to be broken off during the eruption.

4.5 Thin section petrography of the volcaniclastic unit

Seven of the original thin sections, D-(3.2-10.3)-12-E, were from the volcaniclastics and are described below from observations in polarized light microscope and SEM EDX analysis. In general, the composition of the volcaniclastic grains corresponds to swelling clay minerals formed from the degradation of the original ash and lapilli glass. In all thin sections where grains could be seen they are angular to sub rounded.

One thin section was studied from subunit 1, D-3.2-12-E (Fig. 5C). Most of the sample consists of swelling clay minerals originating from the alteration of the volcaniclastic grains. The difference to other studied thin sections is that these clay minerals make up a heterogenous mass without a clear texture. Due to this no proper naming of the sample could be reached. However, a few vague grain boundaries can be seen, with little of the original texture remaining within said grains except for a handful of cement filled vesicles and even fewer contours of degraded mafic mineral. Several non-volcanic, sub rounded grains can be seen clearly and are composed of quartz, K-feldspars or a combination of the two.

Thin section D-4.3-12-E (Fig. 5D) from subunit 2, shows a clear volcaniclastic texture as a clast supported lapilli-tuff. Both ash and lapilli grains contain numerus vesicles filled with a clear cement. The cement is dominated by calcite, but some smaller vesicles are filled with alteration products from the grains. The intergranular cement is dominated by calcite that enclose most grains and fills up all except the largest pore spaces, which instead is filled with kaolinite clay (Fig. 19A).

Two thin sections were produced from subunit 3, D-5.4-12-E and D-7.2-12-E (Fig. 5E-F). These have the same general texture as thin section D-4.3-12-E in subunit 2, only clearer due to a high contrast between grains and cement and due to a lesser degree of degradation. The

first thin section coming from the lower part of the subunit is only cemented with iron rich calcite in both the vesicles and the intergranular spaces. The second thin section coming from the middle part of the subunit has several different kinds of cement. In the vesicles, calcite is still the dominant cement, but chlorite and different zeolites were also identified (Fig. 19B). The chlorite either fills smaller vesicles or occurred as a rim in larger vesicles filled with zeolites. One of the zeolites seen is the Ba rich type called harmotome. In the intergranular spaces the same kind of occurrence is seen with calcite dominating but here it is possible to see chlorites growing on the calcite and the zeolites filling out the last bit of porosities (Fig. 19C-D).

In subunit 4 there is three thin sections with two from the lower part, D-9.1-12-E and D-8.2-12-E (Fig. 5G-H), and one from the middle part, D-10.3-12-E (Fig. 5I). These have the same general grain size and texture as thin sections from subunits 2-3, although cement mineralogy differs. The first thin section has most of its vesicles filled with calcite but it's not the same dominance as seen in previous parts. Both chlorite and especially zeolites are more common with suspected chlorite zonation in several vesicles. The intergranular cement is dominated by zeolites but calcite do still occur in local patches. Thin section D-8.2-12-E was different in the way it was divided in two clear halves, the upper and the lower half (Fig. 5H). The lower half is dominated by calcite cemented vesicles with some chlorite. The intergranular cement is close to 100 % calcite with a handful of patches that by the naked eye looks pink to dark red but in plane polarised light looks red to brown and most of the time

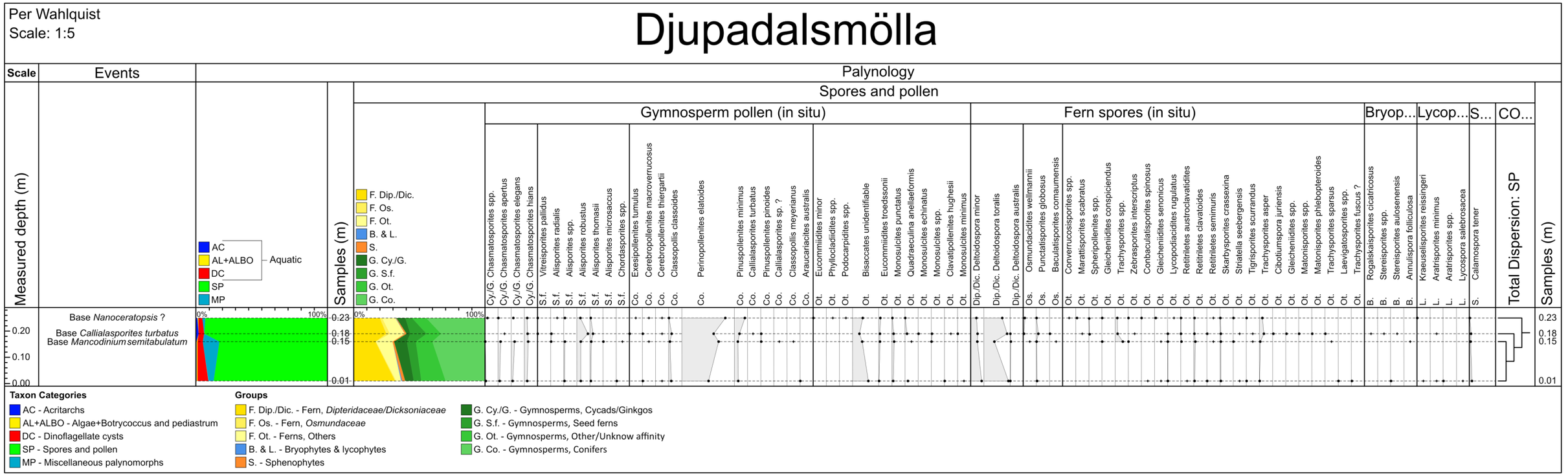

Figure 11. Taxonomic belonging based on Abbink et al. (2004); Petersen & Lindström (2012); Lindström et al. (2017). The conifer pollen Callialasporites turbatus has its first occurrence in the 0.18 m sample and has its FAD in late Pliensbachian.

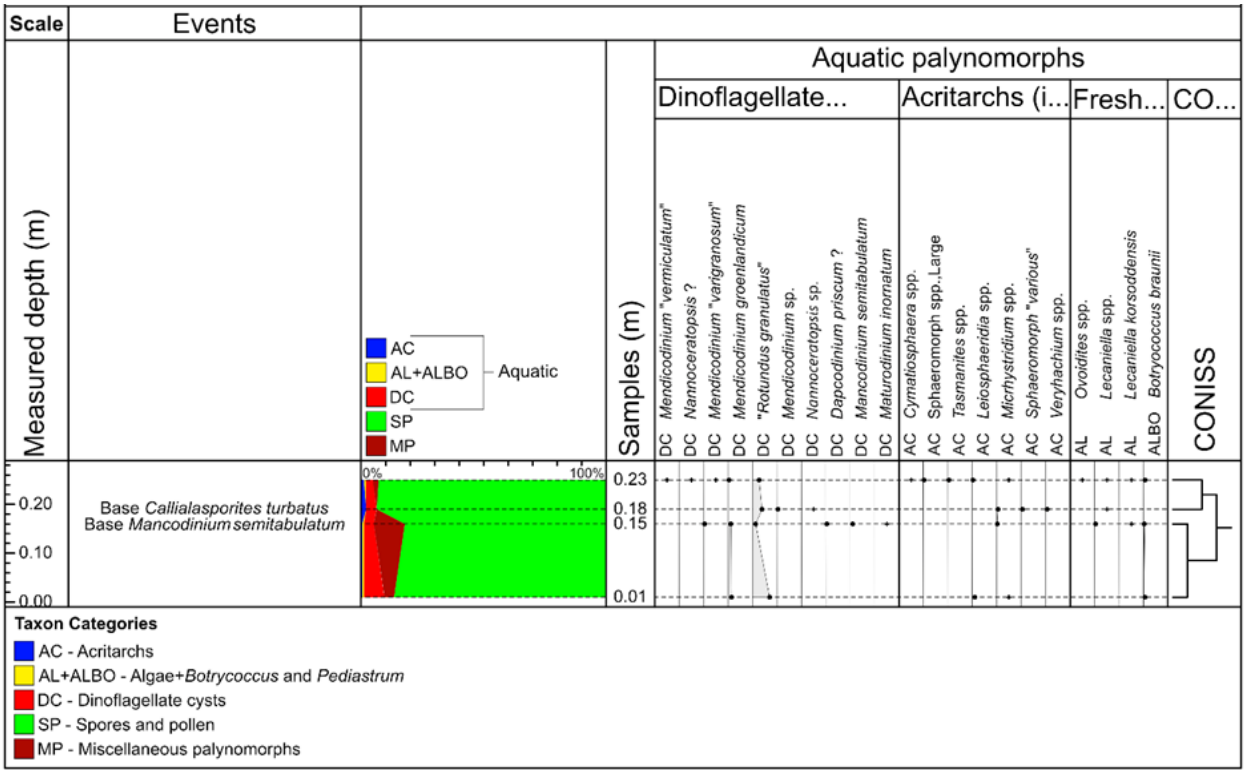

Figure 12. Aquatic palynomorphs. Species indicative for both marine and lacustrine environments were detected in all samples. The first occurrence of the dinoflagellate cyst Mancodinium semitabulatumk is in sample 0.15 m and it has its FAD in late Pliensbachian.

Table 2. Palynomorphs ordered by taxonomic belonging with related plants environmental and climatic preferences as well as photic niches. *based on Abbink et al. (2004); Petersen & Lindström (2012); Lindström et al. (2017). **based on Petersen & Lindström (2012) and Lindström et al. (2017). ***based on Abbink et al. (2004).

Name of palynomorph	**Known or probable parent plant affinity** *	**Habit/ photic niche** **	**Preferred environment** **	**Preferred environment** ***	**Climate** (Abbink et al. 2004)***
Cycads/Ginkgos					
Chasmatosporites spp.		Upper canopy	Mire	Lowland	Drier, cooler
Chasmatosporites apertus		Upper canopy	Mire	Lowland	Drier, cooler
Chasmatosporites elegans		Upper canopy	Mire	Lowland	Drier, cooler
Chasmatosporites hians		Upper canopy	Mire	Lowland	Drier, cooler
Seed fern (Pteridospermatophyta/Pteridosperms)					
Vitreisporites pallidus	Caytoniales	Mid canopy	Mire, riverbanks	River	
Alisporites radialis	Corystospermales	Upper canopy	Mire		
Alisporites spp.	Corystospermales	Upper canopy	Mire		
Alisporites robustus	Corystospermales	Upper canopy	Mire		
Alisporites thomasii	Corystospermales	Upper canopy	Mire	Tidally influenced	
Alisporites microsaccus	Corystospermales	Upper canopy	Mire		
Chordasporites spp.	Corystospermales				
Conifer					
Exesipollenites tumulus	Cupressaceae/ Taxodiaceae	? Upper canopy	Mire	Lowland(coastal)	Drier, warmer
Cerebropollenites macroverrucosus		Upper canopy	Well drained	Pioneer	
Cerebropollenites thiergartii		Upper canopy	Well drained	Pioneer	
Classopollis classoides	Cheirolepidiaceae	Upper canopy	Well drained, coastal		
Perinopollenites elatoides	Cupressaceae/ Taxodiaceae	Upper canopy	Mire, riverbanks	Lowland	Wetter, cooler
Pinuspollenites minimus	Pinaceae	Upper canopy	Well drained		
Callialasporites turbatus	Araucariaceae			Coastal	Cooler
Pinuspollenites pinoides	Pinaceae	Upper canopy	Well drained		
Callialasporites sp. ?	Araucariaceae			Coastal	Cooler
Classopollis meyerianus	Cheirolepidiaceae	Upper canopy	Well drained, coastal		
Araucariacites australis	Auracariaceae	Upper canopy	Well drained, coastal	Coastal	Cooler

Cycads/Ginkgos/Bennettitales/Peltaspermales (Seed ferns)					
Phyllocladiidites spp. (Conifer?)		? Upper canopy			
Podocarpidites spp. (Conifer?)	Podocarpaceae	? Upper canopy			
Bisaccates unidentifiable (Conifer?)		? Upper canopy		Upland?	
Monosulcites punctatus (Cycads/Ginkgos?)		Upper canopy	Mire, drier patches	Lowland	Drier, warmer
Quadraeculina anellaeformis		? Upper canopy	unknown habit	Upland	
Monosulcites "echinatus" (Cycads/Ginkgos?)		Upper canopy	Mire, drier patches	Lowland	Drier, warmer
Monosulcites spp. (Cycads/ Ginkgos?)		Upper canopy	Mire, drier patches	Lowland	Drier, warmer
Clavatipollenites hughesii (Angiosperm???)		? Mid canopy	Unknown habitat	Lowland	Drier, warmer
Erdtmanithecales					
Eucommiidites minor	Erdtmanithecales	? Mid canopy	Mire		
Eucommiidites troedssonii	Erdtmanithecales	? Mid canopy	Mire	Lowland	Drier, warmer
Bennettitales					
Monosulcites minimus	Bennettitales	Mid canopy	Mire	Lowland	Drier, cooler
Fern					
Deltoidospora minor	Dipteridaceae, Dicksoniaceae	Understory	Mire, drier patches	Lowland	Drier, warmer
Deltoidospora toralis	Dipteridaceae, Dicksoniaceae	Understory	Mire, drier patches	Lowland	Drier, warmer
Deltoidospora australis	Dipteridaceae, Dicksoniaceae	Understory	Mire, drier patches	Lowland	Drier, warmer
Osmundacidites wellmannii	Osmundaceae	Ground cover	Mire	Lowland	Wetter, warmer
Punctatisporites globosus	Osmundaceae	Ground cover	Mire	Lowland	Wetter, warmer
Baculatisporites comaumensis	Osmundaceae	Ground cover	Mire	Lowland	Wetter, warmer
Converrucosisporites spp.		Ground cover	Mire		
Marattisporites scabratus	Marattiales	Ground cover	Mire		
Spheripollenites spp.			Mire		
Gleicheniidites conspiciendus	Gleicheniaceae	Ground cover	Mire, drier patches	Lowland	Drier, warmer
Trachysporites spp.		Ground cover	Mire		
Zebrasporites interscriptus		Ground cover	Mire		
Striatella seebergensis	Polypodiaceae	Ground cover	Mire		
Gleicheniidites senonicus	Gleicheniaceae	Ground cover	Mire, drier patches	Lowland	Drier, warmer
Conbaculatisporites spinosus		Ground cover	Mire		
Lycopodiacidites rugulatus		Ground cover	Mire	River	
Retitriletes austroclavatidites		Ground cover	Mire	Tidally influenced	
Retitriletes clavatoides		Ground cover	Mire	Tidally influenced	
Retitriletes semimuris		Ground cover	Mire	Tidally influenced	
Skarbysporites crassexina		Ground cover	Mire		
Tigrisporites scurrandus		Ground cover	Mire	Lowland	Drier, warmer
Trachysporites asper		Ground cover	Mire		
Gleicheniidites spp.	Gleicheniaceae	Ground cover	Mire, drier patches	Lowland	Drier, warmer
Matonisporites spp.	Matoniaceae	Ground cover	Mire	Lowland	Drier, warmer
Matonisporites phlebopteroides	Matoniaceae	Ground cover	Mire	Lowland	Drier, warmer
Cibotiumspora juriensis		Ground cover	Mire		
Trachysporites sparsus		Ground cover	Mire		
Laevigatosporites spp.	Marattiales	Ground cover	Mire		
Trachysporites fuscus ?		Ground cover	Mire		
Bryophyte					
Rogalskaisporites cicatricosus		Ground cover		River	
Stereisporites spp.		Ground cover	Mire	River	
Stereisporites aulosenensis		Ground cover	Mire	River	
Annulispora folliculosa		Ground cover	Mire	River	
Lycophyte					
Kraeuselisporites reissingeri		Ground cover	Mire	River	
Aratrisporites minimus		Ground cover	Mire, coastal	River	
Aratrisporites spp.		Ground cover	Mire, coastal	River	
Lycospora salebrosacea		Ground cover	Mire	River	
Equisetales					
Calamospora tener		Ground cover	Mire, riverbanks	River	

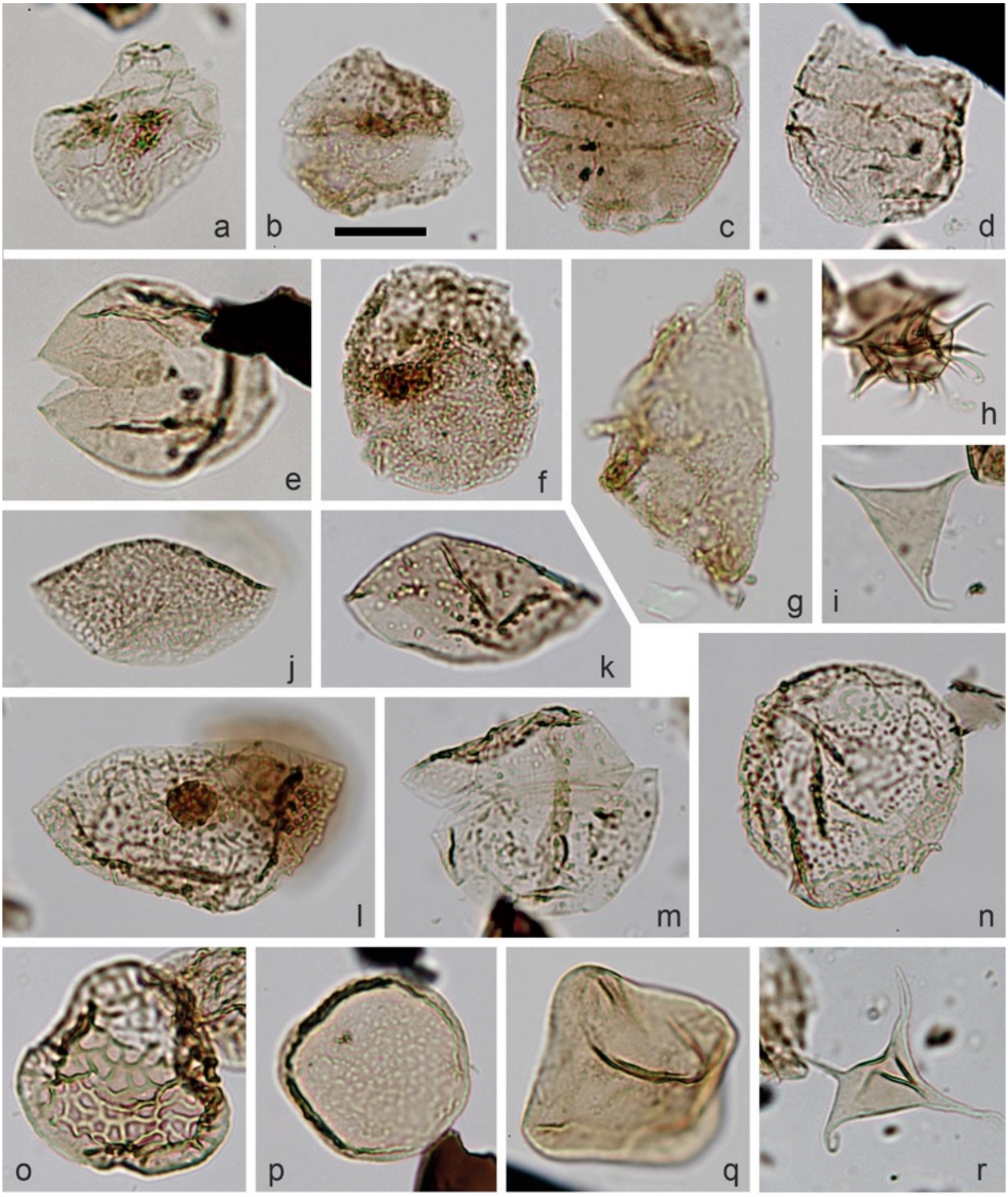

Figure 13. Selected dinoflagellate cysts, acritarchs and freshwater microalgae from Djupadalsmölla followed by sample and slide number as well as England Finder coordinates. Same scale in all pictures with scale bar being 20 µm. a) Unknown dinocyst, 20.33m:5, J47/2. b) "*Rotundus granulatus*", 20.48m:5, H54/3. Note pore plug and slightly constricted paracingulum. c) *Dapcodinium priscum*, 20.33m:4, D29/3. Probably reworked. d) *Dapcodinium priscum*, 20.24m:5, D32/1. Probably reworked. e) *Mendicodinium groenlandicum*, 20.24m:8, P30/1. f) "*Rotundus granulatus*", 20.48m:5, C36/3. Note pore plug. g) ? *Nannoceratopsis* sp., 20.24m:8, J29/3. Poorly preserved specimen. h) *Micrhystridium* sp., 20.48m:5, H26/3. i) *Veryhachium* sp., 20.33m:3, K26/1. j) *Mendicodinium reticulatum*, 20.48m:5, N53/2. Epicyst only. k). *Mendicodinium* sp. cf. *morgenrothum*, 20.48m:5, O38/2. Epicyst only. l) Mendicodinium sp. cf. morgenrothum, 20.48m:5, N35/3. Hypocyst only. m) Mendicodinium sp., 20.48m:5, O55/2. n) *Mendicodinium* sp., 20.48m:5, C26/3. o) *Lecaniella korsdoddensis*, 20.33m:5, J31/1. p) *Lecaniella* sp., 20.24m:8, F30/1. q) *Tetraporina tetragona*, 20.48m:5, K43/3. r) *Veryhachium* sp., 20.24m:5, E57/1.

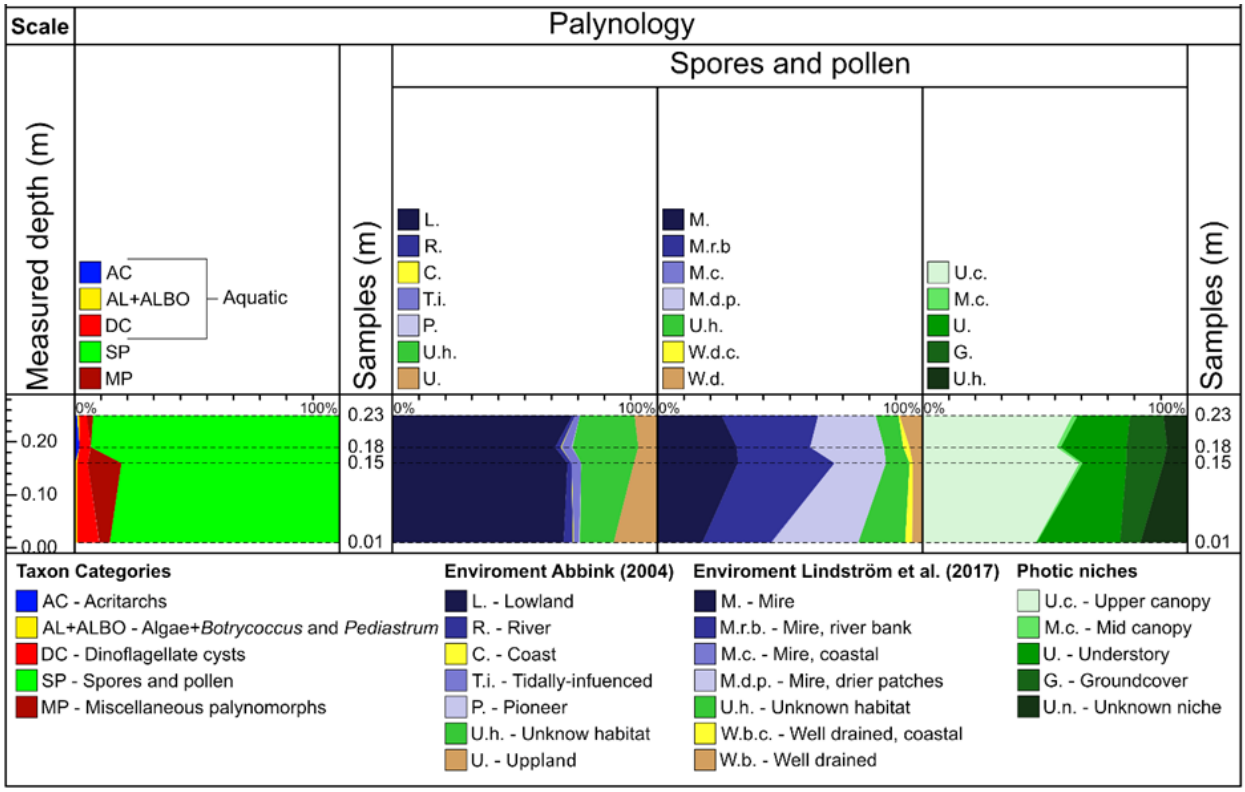

Figure 14. Pollen related plants environmental preferences and photic niches based on Abbink et al. (2004); Petersen & Lindström (2012); Lindström et al. (2017). The pollen belonging to each group can be seen in Table 2.

has a radiating shape (Fig. 17B, 19E). These patches consist of Fe rich calcite interfingered with Ca rich siderite. In the upper part, the cement in the vesicles is still calcite with some chlorite but the intergranular cement is 100 % zeolite (Fig. 19F). Thin section D-10.3-12-E from middle part of the subunit has once again a dominance of calcite cemented vesicles, some chlorite filled with possible zonation, and some filled with zeolites. The intra-granular cement is also dominated by calcite, but some zeolite patches do occur as well as some dark streaks most likely consisting of Ca rich siderite.

The five samples used for point counting, D-(4.3-5.4, 7.2-8.2, 10.3)-12-E, show a similar result with none of them deviating significantly in terms of grain size or intragranular porosity as can be seen in the log. Ash grains varies between 43-48 % while lapilli grains varies between 19-25 %. The intergranular cement ranges from 27-36 %. When cement filled vesicles were encountered, they were counted as part of the grain they were found in.

A single sample, D-4.3-12-E, were also used to calculate porosity before cementation. Both intra- and intergranular cement were counted and gave a total porosity of 46% with the intragranular porosity being 16% and the intergranular porosity being 30%.

5 Discussion

5.1 The sub-Jurassic weathering surface

As Pangea started to break up in the Triassic (Kimmerian rifting), many of the faults in the STZ got reactivated (Vejbæk 1990; Mogensen 1994; Mogensen 1995; Michelsen 1997; Erlström 2020). This formed new local depocenters in Skåne and surroundings through much of the early Mesozoic. As these faults settled again and sedimentation gradually filled up the smaller depocenters the sedimentation moved further and further on to the Skåne part of the STZ, which in much of the Mesozoic and later times likely acted as a relative high compared to much of the Tornquist fan.

In the latest Triassic and earliest Jurassic, the climate and sedimentation of the region changed drastically from a warm and dry environment dominated by alluvial fan deposits in the Norian to a wet and humid climate during the Rhaetian with deposition of more intensely weathered sediments, palaeosols, coals and mineralogically mature sandstones (Ahlberg et al. 2002). The sedimentation also started to reach even further into Skåne with many larger transgressions taking place from the Rhaetian and onwards (Nielsen 2003; Lindström & Erlström 2006), as deeply weathered crystalline basement rocks in the central parts of Skåne started to get kaolinized weathered and/or covered with siliciclastic sediments. In the northwest of Skåne, tidal flats dominated, depositing a mix of clay and sand with sporadic coal deposits, while the central parts were more energetic and therefor depositing cleaner quartz sand and locally monomict quartz conglomerates. In the north and northeast of Skåne, and likely on some of the horsts as well, the weathered felsic basement rocks were still exposed. This caused the formation of the sub-Jurassic weathering surface and the associated kaolinite weathering of the crystalline basement.

The high degree of chemical weathering at the top of the crystalline basement, the sharp transition to the overlying dark mudstone and, most importantly, the fact that almost two meter of material was washed out at the transition between the two units, indicate even

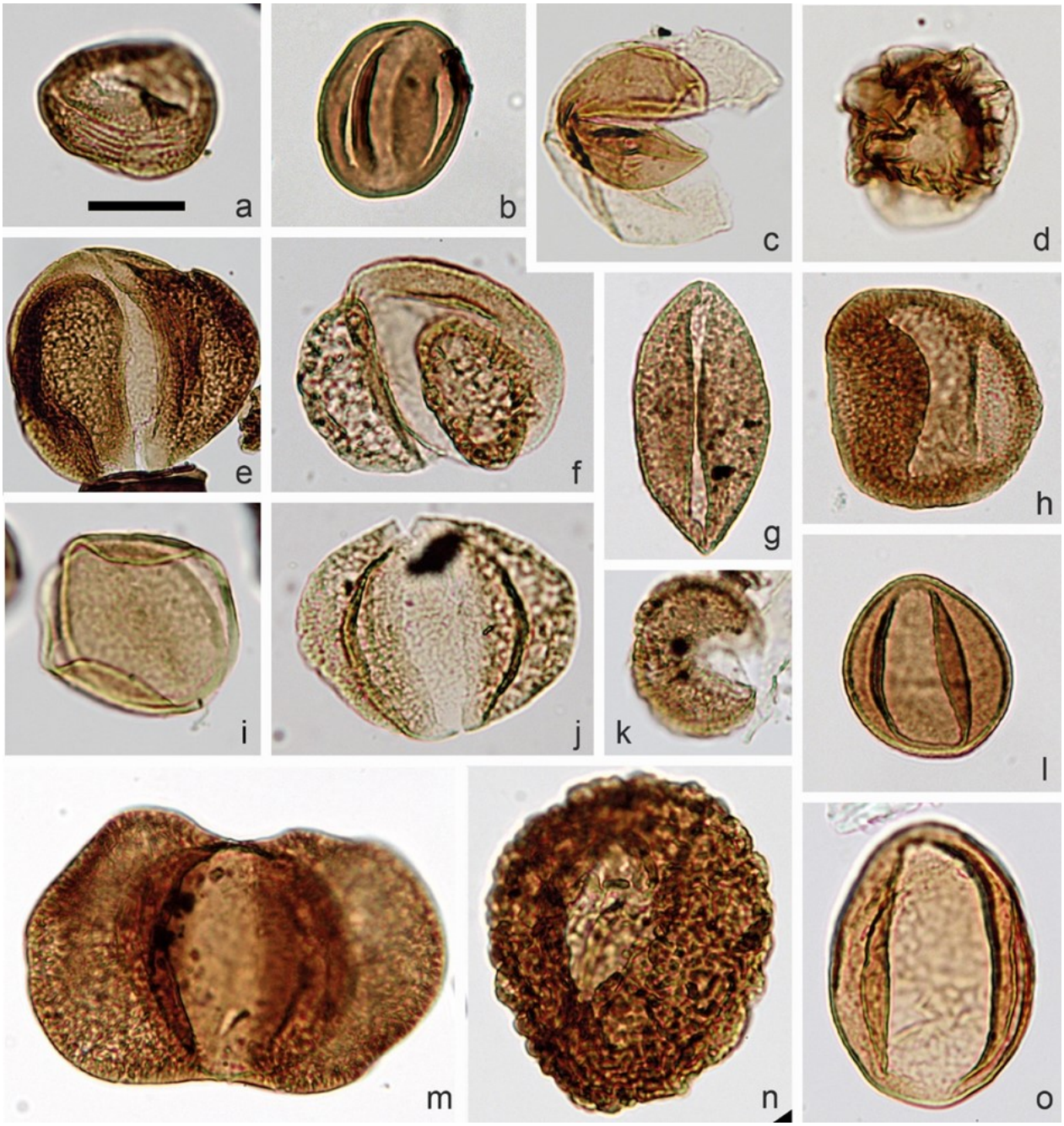

Figure 15. Selected pollen taxa from Djupadalsmölla, followed by sample and slide number as well as England Finder coordinates. Same scale in all pictures with scale bar being 20 µm. a) *Classopollis classoides*, 20.48m:5, G49/1. b) *Eucomiidites troedsonii*, 20.24m:9, K28/2. c) *Perinopollenites elatoides*, 20.33m:5, G47/4. d) *Callialasporites dampieri*, 20.24m:5, C30/3. e) *Alisporites thomasii*, 20.24m:9, N29/1. f) *Pinuspollenites minimus*, 20.24m:5, C33/1. g) *Monosulcites punctatus*, 20.24m:9, L44/1. h) *Quadraeculina anellaeformis*, 20.24m:5, C54/1. i) *Lecaniella* sp., 20.48m:5, P19/4. j) *Alisporites thomasii*, 20.48m:5, O56/4. k) *Clavatipollenites hughesii*, 20.24m:8, E39/2. l) *Chasmatosporites apertus*, 20.48m:5, E40/4. m) *Alisporites radialis*, 20.48m:5, J28/2. n) *Cerebropollenites macroverrucosus*, 20.48m:5, G49/1. o) *Chasmatosporites elegans*, 20.24m:9, F33/4.

more weathered material to have been present, likely consisting of clean kaolinite and possibly also mudstone. Chemical weathering is dependent on water and favoured by high temperatures. The substantial weathering of the crystalline basement at Djupadalsmölla cannot be the result of pre-Rhaetian weathering, due to the dry climate at the time (cf. Ahlberg et al. 2003). Hence the weathering must have taken place sometime between the Rhaetian and the late Pliensbachian, as implied by the palynomorph age in the overlying mudstone; that is, over a time period of maximum 25 Ma.

5.2 The establishment of an aquatic environment

The dark-coloured mudstone at the top of the basement rocks were deposited in an aquatic environment (Figs. 6-7). The temporal changes in the composition of this unit, with interbedded layers of organic-rich clay/silt and fine-grained sand, suggest that the energy within this aquatic environment fluctuated due to the

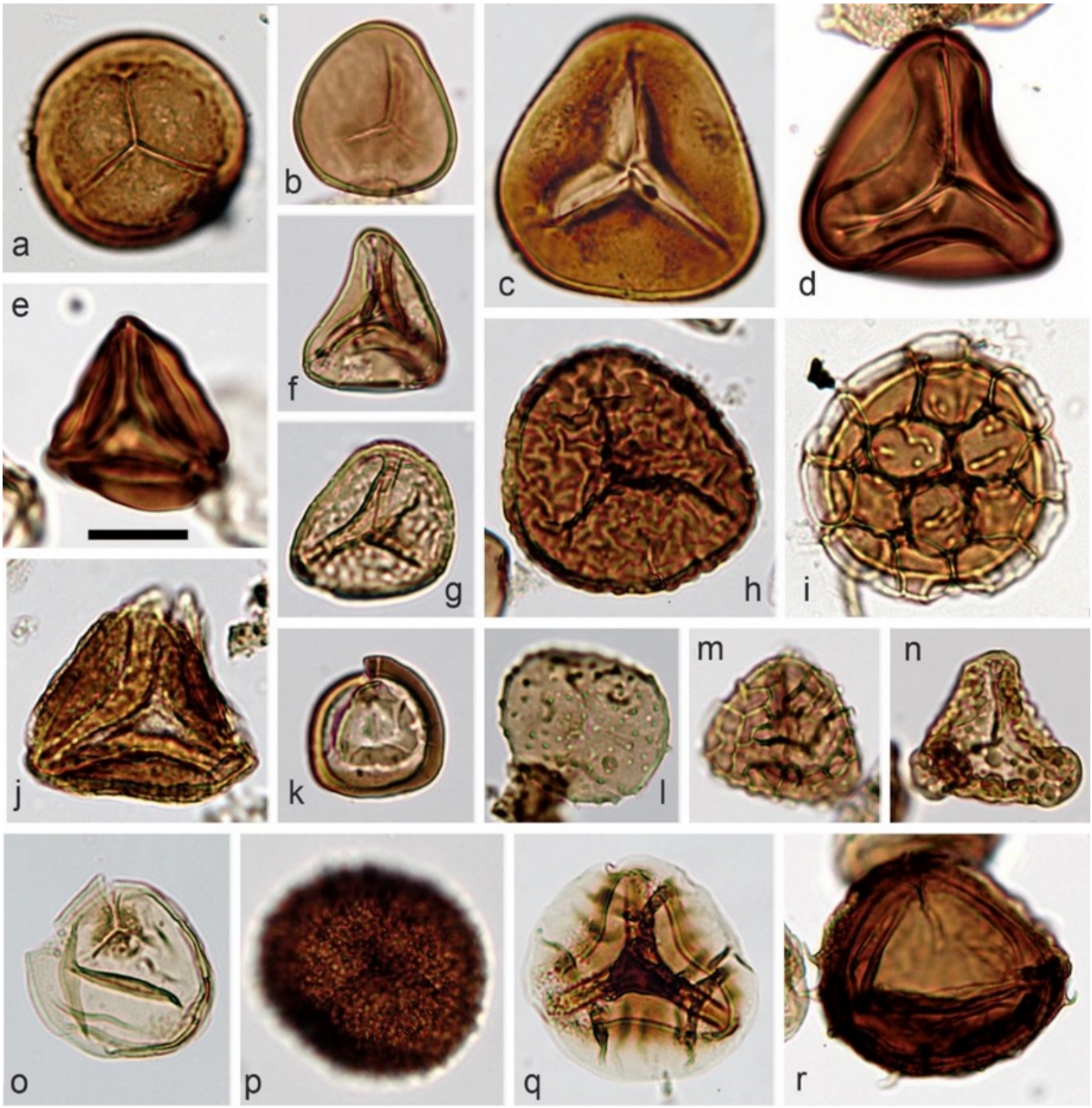

Figure 16. Selected spores from Djupadalsmölla, followed by sample and slide number as well as England Finder coordinates. Same scale in all pictures with scale bar being 20 µm. a) *Punctatisporites globosus*, 20.24m:5, F39/4. b) *Deltoidospora minor*, 20.24m:8, F30/1. c) *Deltoidospora australis*, 20.48m:5, P20/2. d) *Deltoidospora toralis*-type, large specimen, 20.48m:4, C30/3. e) *Gleicheniidites senonicus*, 20.48m:5, L26/3. f) *Deltoidospora toralis*, 20.24m:8, J33/2. g) *Stereisporites aulosenensis*, 20.33m:5, M23/3. h) *Lycopodiacidites rugulatus*, 20.48m:5, K44/1. i) *Retitriletes clavatoides*, 20.24m:5, E58/1. j) *Gleicheniidites conspiciendus*, 20.48m:5, P47/2. k) *Dicyclosporis* sp., 20.24m:9, L43/1. l) *Foraminisporis jurassicus*, 20.48m:5, Q32/3. m) *Retitriletes semimuris*, 20.48m:5, K35/3. n) cf. *Manumia delcourtii*, 20.48m:5, H27/1. o) *Calamospora tener*, 20.33m:5, P24/3. p) *Baculatisporites comaumensis*, 20.24m:8, P30/1. q) *Zebrasporites interscriptus*, 20.33m:5, P25/4. r) *Kraeuselisporites reissingerii*, 20.48m:5, J54/1.

presence of weak currents. The relative common occurrence of dinoflagellate cysts in all four samples implies that there were marine influences on this environment. However, the presence of a range of algae, indicative of calm lacustrine to brackish environments, rule out a fully marine setting. Given the pronounced topography of the underlying basement surface, this was possibly a restricted area, such as a lagoon or protected bay.

The occurrence of the palynomorphs *Callialasporites turbatus*, *Mancodinium semitabulatum* and *Nannoceratopsis gracilis* gives a maximum age of late Pliensbachian with all three palynomorphs having their FAD there (Batten & Koppelhus 1996; Poulsen & Riding 2003). The fact that we do not find any *Parvocysta*, *Phallocysta* and *Susadinium* dinoflagellate cysts and/or common occurrences of *Callialasporites* pollen, is a strong indication that we are not in the Toarcian but instead in the late Pliensbachian (Batten & Koppelhus 1996; Van De Schootbrugge et al. 2020).

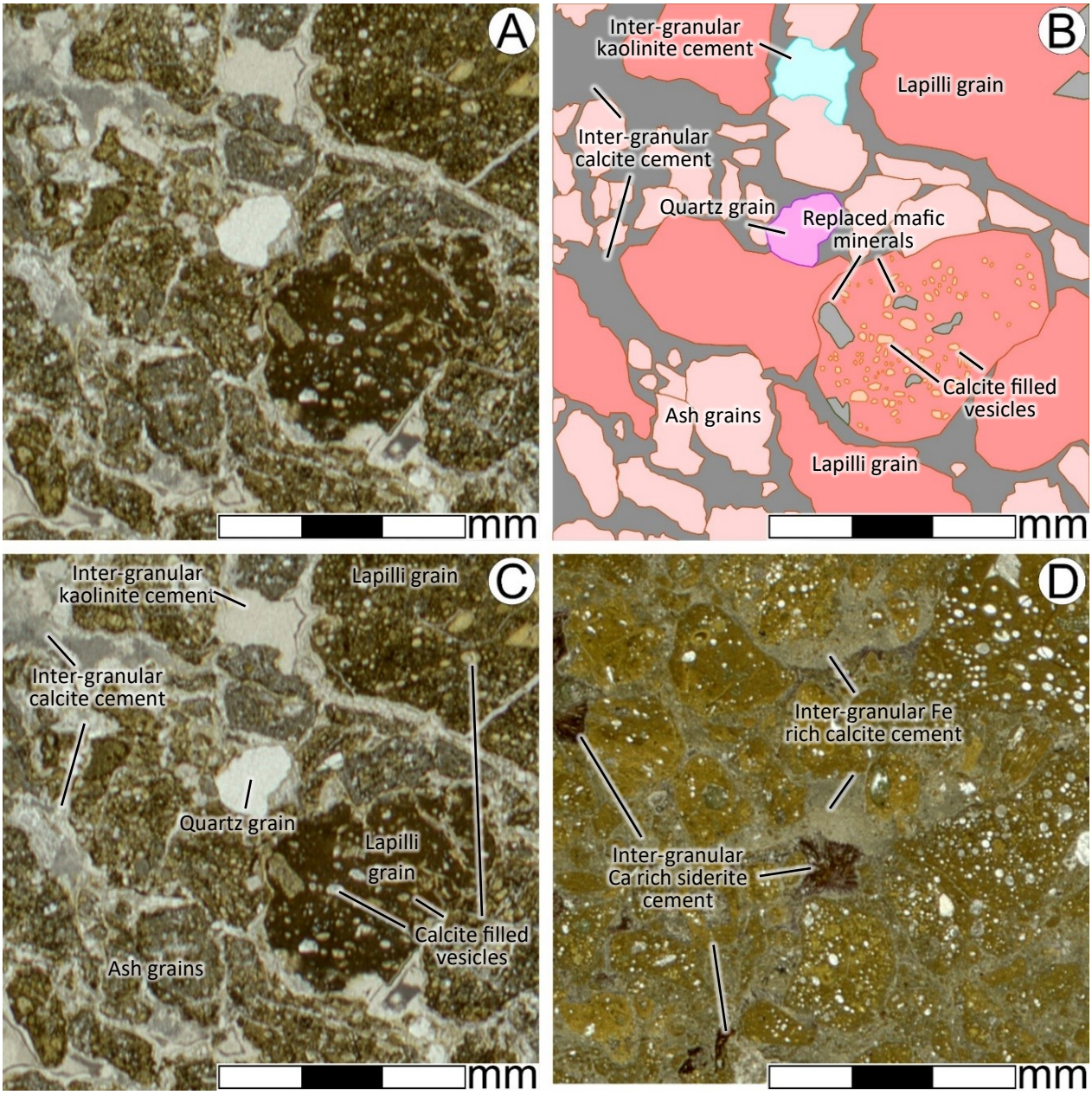

Figure 17. Thin sections presenting an overview of the descriptive microscopic texture and volcaniclastic terminology used. Close up pictures of the thin section D-4.3-12-E and D-8.2-12-E, (Fig. 5D, H). A-B) Thin section and sketch showing an unusually well-preserved texture of the lapilli-tuff at Djupadalsmölla. Note larger lapilli grains with abundant calcite-filled vesicles enclosed in a finer ash matrix. The light red in the sketch represents the ash grains (< 2 mm). The darker red represents the lapilli grains (> 2 mm) and the grey represents intergranular cement or veins filled with cement. Purple is a sub rounded quartz grain and light blue represents a small patch of kaolinite cement. The vesicles (orange) were only added to one lapilli grain but have a similar distribution in the other volcanic grains. Replaced mafic minerals (grey with dark green boarder) can be seen in two of the grains but are likely to have occurred in many more. It is hard to distinguish these from vesicles, fissure and/or other alterations seen in the grains. C is a combination of A and B. D) This sample is more typical for the core succession due to degradation through clay weathering and a more even texture. Two different types of cement occur, with the dominating cement being Fe rich calcite. The small darker patches are Ca rich siderite interfingering with the Fe rich calcite. 20.24m:9, F33/4.

The vegetation composition derived from the palynomorph analysis support a humid and intermediately warm climate with plants preferring both cooler (*Perinopollenites elatoides* & *Chasmatosporites* spp. etc.) and warmer (Monosulcites spp. & Deltoidospora toralis etc.) climate (Abbink et al. 2004; Table. 2). It also gives a picture of a wetter low-land vegetation with the dominant pollen occurrence being *Perinopollenites elatoides* which comes from a Taxodiaceae (swamp cypress; Figs. 12-14). The parent plant of *P. elatoides* is known to have preferred wetter conditions, such as rivers or wetlands, giving evidence for the lacustrine influence on the area while the sparse occurrence of *Classopollis* give an indication that conditions were not optimum for the parent plants of these types of pollen. With the dominant environment derived from the interpretation of Abbink et al. (2004) being lowland and the three dominant environments

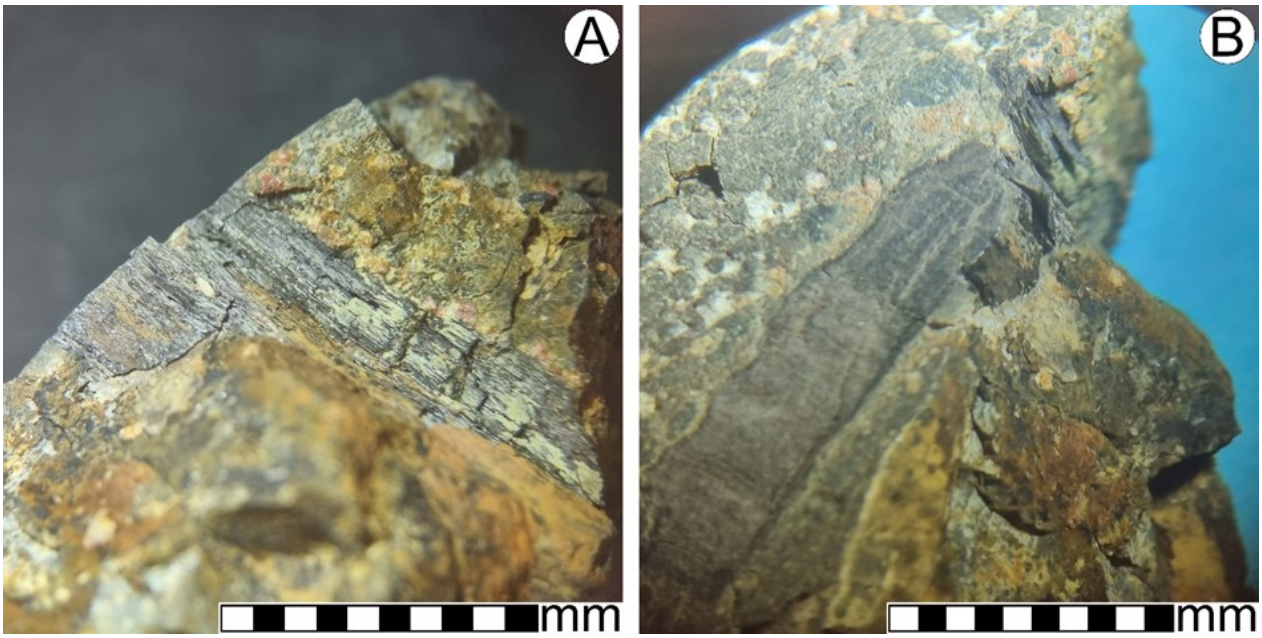

Fig. 18. Petrified wood with preserved fibrous structures from +10.85 m in subunit 3 of the volcaniclastic unit.

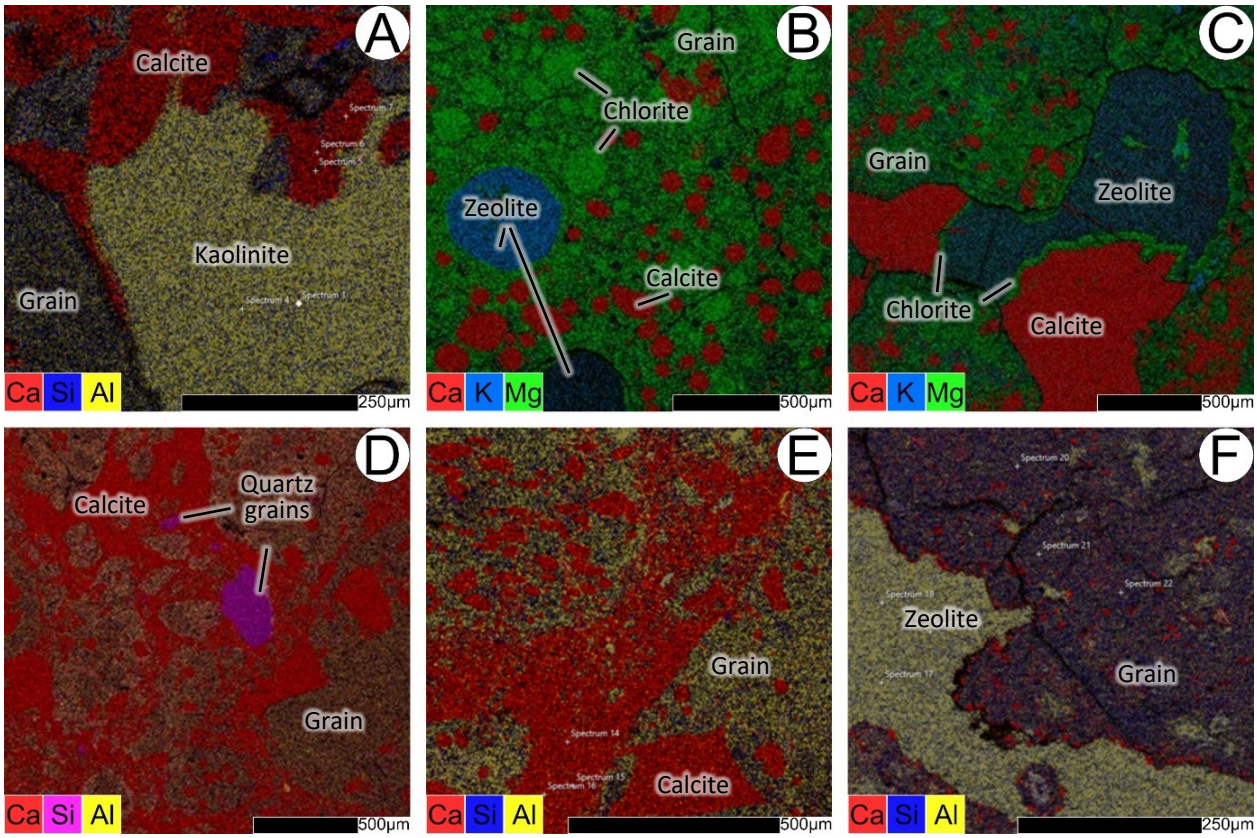

Figure 19. Elemental maps from EDX analysis on pyroclastic thin sections showing clear structures and different cement fillings. A) D-4.3-12-E, subunit 2, ca +0.60 m. Intergranular calcite cement enclosing the volcaniclastic grains with secondary kaolinite cement filling up the remaining intergranular porosity. B-D) D-7.2-12-E, subunit 3, ca +7.30 m. In B several vesicles with calcite, chlorite and two larger vesicles with zeolite cement were noted. The lower one of the two zeolite vesicle reaches towards the Ba endmember of zeolite, harmotome. In C, three different generations of intergranular cement can be seen with a first generation of calcite, followed by a thin layer of chlorite and lastly filled out with zeolite. In D a larger and smaller quartz grain occur alongside the volcaniclastic grains. E-F) D-8.2-12-E, subunit 4, ca +15.60 m. In E the typical calcite cement composition can be seen in the lower part of the sample, while in F, the upper part, the zeolite cement has taken over as the only intergranular cement with calcite still cementing the vesicles.

derived from the interpretations of Petersen & Lindström (2012) and Lindström et al. (2017) was, mire (15-28% tpc), mire/riverbanks (22-34% tpc) and mire/drier patches (16-28% tpc; Fig. 14). This suggests a wet lowland in and around the area with somewhat limited topography.

Eight out of the total eleven reworked palynomorphs were found in the uppermost sample of the mudstone, suggesting more erosion of older strata in the surrounding area during this time. The proportion of reworked material is however low for this rock type in early Jurassic of Skåne (Guy-Ohlson et al. 1987; Lindström et al. 2017). The unusually dark pollen grains that do not differ in age from the remaining palynoflora in the top sample could possibly indicate burning from a forest fire (personal communication Sofie Lindström 2021).

5.3 Volcanism

The first clear signs of the volcanic activity in the core comes from the volcanic clasts pressed into the top of the dark-coloured mudstone unit. The clasts are embedded in the topmost part of the mudstone implying that the mudstone was still unconsolidated when the clasts were deposited. This strongly supports the idea of the mudstone and volcaniclastics being of the same age, namely late Pliensbachian. This is in good agreement with the nearby basalt outcrop of Eneskogen and Jällabjär, 1 and 3 km away, dated to 182.1 ± 0.6 and 183.5 ± 0.8 Ma, respectively (Bergelin 2009).

The finer details of the eruption or if it was several eruptions are difficult to resolve. The lack of clear bedding features, sedimentary structures or fabrics make interpretation of depositional processes difficult. The succession is overall homogenous and there are no evidence for repeated eruptions of different composition. Notable is the more than twenty pieces of preserved wood implying eruption, transportation and deposition across forested areas. Another feature is the small grains of quartz and K-feldspars that are embedded in the matrix and cement with the other grains (see also Augustsson (2001)). The grains are so small that it is unlikely that they would be picked up from the wall rock but instead have been picked up on the surface. Grain of the same type and size are also found in the topmost sample of the mudstone supporting the fact that these comes from the surface. The only two depositional processes that fit all these descriptions are pyroclastic flows, and lahars (Fisher & Schmincke 1984; McPhie et al. 1993). A pyroclastic flow is a surge of hot gases and volcaniclastic material that follows the topography of the landscape and forms a direct deposition in low lying areas. A lahar on the other hand is a redeposition process that take place when previously deposited volcaniclastic material gets remobilised by water as a mass movement and just as the pyroclastic deposit follows the topography to low lying areas. Lahars are commonly taking place shortly after eruptions before vegetation can stabilise the ground. Both processes could pick up the wooden material as well as the accidental lithics and would explain the fine-grained quartz grains in the rock. The distance for the deposition or the redeposition would likely be quite short as during longer transport a higher degree of sorting and rounding is usually achieved. If the volcaniclastics came from a strombolian eruption in the form of a scoria cone as suggested by Augustsson (2001), and the eruption was located at either Eneskogen or Jällabjär both processes could explain the deposit at Djupadalsmölla.

As the first subunit, 0.25-0.45 m, is both pushed into the mudstone and more degraded (Figs. 4-5D), it is likely that the area was at least wet or partly covered by water. The water body must however have been rather small/shallow and have a low energy level to not sort and round of the grains.

5.4 Post-volcanic events

The calculated intergranular porosity of 27-36% and the total porosity of 54% in sample D-4.3-12-E supports limited compaction and thus early lithification of the strata at Djupadalsmölla. This conclusion was also reached by Augustsson (2001). Four or five different types of cement are documented. In samples D-4.3-12-E and D-7.2-12-E it is possible to note the order. As calcite is the first cement to form in both samples and grow on the grains with kaolinite coming second in D-4.3-12-E and chlorite coming second in D -7.2-12-E with zeolite precipitating last. The finding of Ba rich zeolites like harmotome both in this study and in the study by Augustsson (2001) gives strong evidence that a subsequent marine transgression affected the diagenesis. The reason for this is that seawater is a major source of barium and, as discussed in the previous part, only a very shallow water body must have been present during the deposition.

Two other events that are hard to place in the chronology of the site is the tilting and micro faulting of the mudstone. Both could have taken place before the volcanism, but this is highly unlikely as the same angled tilt can be seen in features of the volcaniclastics at the outcrop. More likely is that the movements took place either during the volcanism as the forces from the incoming volcaniclastics might have affected the mudstone or after as results from fault movements in the STZ during the Mesozoic.

6 Conclusions

The studied strata in the Djupadalsmölla drill core can be subdivided in three rock units; a kaolinite-weathered crystalline basement overlain by a thin mudstone unit rich in palynomorphs and volcaniclastic strata.

A late Pliensbachian age is suggested from the co-occurrence of rare Callialasporites turbatus, Mancodinium semitabulatum and Nannoceratopsis gracilis, but also the absence of Parvocysta, Phallocysta and Susadinium dinoflagellate cysts and/or common occurrences of Callialasporites pollen.

The environment in Djupadalsmölla in the late Pliensbachian was a warm humid climate in a lagoon or protected bay with both marine and lacustrine influences. A thick forest cover dominated by swamp cypresses, other conifers, ginkgoes, and seed ferns spread out in the sky and a thick understory/ground cover with different kinds of ferns covering the ground.

The volcaniclastic deposit in Djupadalsmölla is a massive, calcite cemented lapilli tuff, partly replaced

by swelling clay minerals. Minor cementation of zeolites, chlorite, Fe rich calcite and Ca riche siderite also occur. The stratigraphic changes in colours and degree of lithification are most likely related to diagenetic processes. The depositional process that formed the deposit in Djupadalsmölla have been suggested to be both a pyroclastic flow (Augustsson 2001) and a lahar (Norling et al. 1993; Wikman & Sivhed 1993). Both are likely and no evidence to rule out one or the other have been reached in this study. It is however clear that the transport distance from the source was very short and the nearby basalt outcrops at Eneskogen and Jällabjär are the most likely sources or having the same source due to concordant ages of around 183 Ma (late Pliensbachian) and the distance.

7 Acknowledgements

Thank you to my supervisor Mikael Calner and co-supervisor Ulf Söderlund, for much support and good discussions since the beginning of the project. Without this support, the project would not have been possible to complete. Big thank you to my co-supervisor Sofie Lindström for the immense help with everything related to palynomorphs, as well as general input on many other aspects of the project. I also want to thank Carita Agustsson for her early input and insights in the subject and the locality of Djupadalsmölla. Another thanks go to Oliver Lehnert and the team in Erlangen for production of thin sections. I want to thank Anders Lindskog for his help with producing much needed thin sections and for other lab-associated work during the pandemic. A big thanks goes to Märta Westberg and Anna Sartell for helping during SEM. This project would however not been possible without the work of Ingemar Bergelin back in 2012.

8 References

Abbink, O. A., Van Konijnenburg-Van Cittert, J. H. A. & Visscher, H., 2004: A sporomorph ecogroup model for the Northwest European Jurassic - Lower Cretaceousi: concepts and framework. Netherlands Journal of Geosciences - Geologie en Mijnbouw 83, 17-31. doi: 10.1017/s0016774600020436

Ahlberg, A., Arndorff, L. & Guy-Ohlson, D., 2002: Onshore climate change during the Late Triassic marine inundation of the Central European Basin. Terra Nova 14, 241-248. doi: 10.1046/j.1365-3121.2002.00416.x

Ahlberg, A., Olsson, I. & Šimkevičius, P., 2003: Triassic–Jurassic weathering and clay mineral dispersal in basement areas and sedimentary basins of southern Sweden. Sedimentary Geology 161, 15-29. doi: 10.1016/s0037-0738(02)00381-0

Andréasson, P.-G. & Rodhe, A., 1990: Geology of the Protogine Zone south of Lake Vättern, southern Sweden: A reinterpretation. Geologiska Föreningen i Stockholm Förhandlingar 112, 107-125. doi: 10.1080/11035899009453168

Ask, R., 1996: Single zircon evaporation Pb-Pb ages from the Vaggeryd syenite and dolerites in the SE part of the Sveconorwegian orogen, Småland, S Sweden. GFF 118, 8-8. doi: 10.1080/11035899609546267

Augustsson, C., 1999: Lapillituff som bevis för underjurassisk vulkanism av strombolikaraktär i Skåne. Lunds Universitet. 19 pp.

Augustsson, C., 2001: Lapilli tuff as evidence of Early Jurassic Strombolian-type volcanism in Scania, southern Sweden. GFF 123, 23-28. doi: 10.1080/11035890101231023

Batten, D. & Koppelhus, E. 1996: Biostratigraphic significance of uppermost Triassic and Jurassic miospores in Northwest Europe. In,

Bergelin, I., 2009: Jurassic volcanism in Skåne, southern Sweden, and its relation to coeval regional and global events. GFF 131, 165-175. doi: 10.1080/11035890902851278

Bergelin, I. & Calner, M. 2012. Skånsk vulkanism undersöks med nya metoder. Geologiskt forum 76, 22-23.

Bergelin, I., Obst, K., Söderlund, U., Larsson, K. & Johansson, L., 2010: Mesozoic rift magmatism in the North Sea region: 40Ar/39Ar geochronology of Scanian basalts and geochemical constraints. International Journal of Earth Sciences 100, 787-804. doi: 10.1007/s00531-010-0516-3

Bomfleur, B., Grimm, G. W. & Mcloughlin, S., 2015: Osmunda pulchella sp. nov. from the Jurassic of Sweden—reconciling molecular and fossil evidence in the phylogeny of modern royal ferns (Osmundaceae). BMC Evolutionary Biology 15, 126. doi: 10.1186/s12862-015-0400-7

Bomfleur, B., Mcloughlin, S. & Vajda, V., 2014: Fossilized Nuclei and Chromosomes Reveal 180 Million Years of Genomic Stasis in Royal Ferns. Science 343, 1376-1377. doi: 10.1126/science.1249884

Bylund, G. & Halvorsen, E., 1993: Palaeomagnetic Study of Mesozoic Basalts From Scania, Southernmost Sweden. Oxford University Press (OUP). 138-144 pp.

Bölau, E., 1966: Der Tertiäre vulkanismus in zentralschonen, südschweden. Lunds Universitet. 60 p.

Eichstädt, F., 1883: Om basalttuffen vid Djupadal i Skåne. Geologiska Föreningen i Stockholm Förhandlingar 6, 408-415. doi: 10.1080/11035898309444082

Erlström, M. 2020: Carboniferous–Neogene tectonic evolution of the Fennoscandian transition zone, southern Sweden. In M. B. Stephens & J. Bergman Weihed (eds.): Sweden: Lithotectonic Framework, Tectonic Evolution and Mineral Resources, 603-620. Geological Society of London, Geological Society, London, Memoirs.

Ernst, R. & Buchan, K., 1997: Giant Radiating Dyke Swarms: Their Use in Identifying Pre-Mesozoic Large Igneous Provinces and Mantle Plumes. Washington DC American Geophysical Union Geophysical Monograph Series, 297-333. doi: 10.1029/GM100p0297

Fisher, R. V. & Schmincke, H.-U. 1984: Pyroclastic Fragments and Deposits. In R. V. Fisher & H.-U. Schmincke (eds.): Pyroclastic Rocks, 89-124. Springer Berlin Heidelberg, Berlin, Heidelberg.

Guy-Ohlson, D., 1998: The use of the microalga Botryococcus in the interpretation of lacustrine environments at the Jurassic–Cretaceous transition in Sweden. Palaeogeography, Palaeoclimatology, Palaeoecology 140, 347-356. doi: https://doi.org/10.1016/S0031-0182(98)00019-4

Guy-Ohlson, D., Lindqvist, B. & Norling, E., 1987: Reworked Carboniferous spores in Swedish Mesozoic sediments. Geologiska Föreningen i Stockholm Förhandlingar 109, 295-306. doi: 10.1080/11035898709453093

Henning, A., 1902: Basalt-Tuff von Lillö. Centralblatt für Mineralogie Geologie und Paläontologie, 357-362.

Hisinger, W., 1826: Versucheiner mineralogischen Geographie von Schweden, umgearbeitete und vermehrte Auflage. Lepzig.

Hounslow, M. W., Mckie, T. & Ruffell, A. H. 2012: Post-Variscan Interplate Setting. In N. Woodcock & R. Strachan (eds.): Geological History of Britain and Ireland, 2 ed, 300-321. Blackwell Publishing Ltd.,

Jarl, L.-G., 2002: U-Pb zircon ages from the Vaggeryd syenite and the adjacent Hagshult granite, southern Sweden. GFF 124, 211-216. doi: 10.1080/11035890201244211

Klingspor, I., 1976: Radiometric age-determination of basalts, dolerites and related syenite in Skåne, southern Sweden. Geologiska Föreningen i Stockholm Förhandlingar 98, 195-216. doi: 10.1080/11035897609454371

Lindström, S. & Erlström, M., 2006: The late Rhaetian transgression in southern Sweden: Regional (and global) recognition and relation to the Triassic–Jurassic boundary. 241, 339-372. doi: 10.1016/j.palaeo.2006.04.006

Lindström, S., Erlström, M., Piasecki, S., Nielsen, L. H. & Mathiesen, A., 2017: Palynology and terrestrial ecosystem change of the Middle Triassic to lowermost Jurassic succession of the eastern Danish Basin. Review of Palaeobotany and Palynology 244, 65-95. doi: https://doi.org/10.1016/j.revpalbo.2017.04.007

Mcloughlin, S. & Bomfleur, B., 2016: Biotic interactions in an exceptionally well preserved osmundaceous fern rhizome from the Early Jurassic of Sweden. Palaeogeography, Palaeoclimatology, Palaeoecology 464, 86-96. doi: 10.1016/j.palaeo.2016.01.044

Mcphie, J., Doyle, M., Allen, R., University Of, T., Centre for Ore, D. & Exploration, S., 1993: Volcanic textures : a guide to the interpretation of textures in volcanic rocks. Centre for Ore Deposit and Exploration Studies, University of Tasmania, Hobart, Tas.

Michelsen, O., 1997: Mesozoic and Cenozoic stratigraphy and structural development of the Sorgenfrei–Tornquist Zone. Zeitschrift der Deutschen Gesellschaft für Geowissenschaften, 148,33–50 p. doi: 10.1127/zdgg/148/1997/33

Michelsen, O. & Nielsen, L. H., 1993: Structural development of the Fennoscandian Border Zone, offshore Denmark. Marine and Petroleum Geology 10, 124-134. doi: 10.1016/0264-8172(93)90017-m

Mogensen, T. E., 1994: Palaeozoic structural development along the Tornquist Zone, Kattegat area, Denmark. Tectonophysics 240, 191-214. doi: 10.1016/0040-1951(94)90272-0

Mogensen, T. E., 1995: Triassic and Jurassic structural development along the Tornquist Zone, Denmark. Tectonophysics 252, 197-220. doi: 10.1016/0040-1951(95)00110-7

Nathorst, A. G., 1887: Till frågan om de skånska dislokationernas åider. Geologiska Föreningen i Stockholm Förhandlingar 9, 74-130. doi: 10.1080/11035898709442455

Nielsen, L. H., 2003: Late Triassic – Jurassic development of the Danish Basin and the Fennoscandian Border Zone, southern Scandinavia. Geological Survey of Denmark and Greenland (GEUS) Bulletin 1, 459-526. doi: 10.34194/geusb.v1.4681

Norin, R., 1934: Zur Geologie der südschwedischen Basalte.

Norin, R., 1940: Problems concerning the volcanic ash layers of the Lower Tertiary of Denmark. GFF 62, 31-44.

Norling, E., Ahlberg, A., Erlström, M. & Sivhed, U., 1993: Guide to the Upper Triassic and Jurassic geology of Sweden. SGU series Ca. Research paper, 70.

Obst, K. & Katzung, G., 2006: Spatial distribution and emplacement features of Permo-Carboniferous dykes at the southwestern margin of the Fennoscandian Shield. Dyke Swarms - Time Markers of Crustal Evolution - Proceedings of the 5th International Conference, IDC-5, 257-272. doi: 10.1201/NOE0415398992.ch18

Petersen, H. I. & Lindström, S., 2012: Synchronous Wildfire Activity Rise and Mire Deforestation at the Triassic–Jurassic Boundary. PLoS ONE 7, e47236. doi: 10.1371/journal.pone.0047236

Poulsen, N.E., Gudmundsson, L., Hansen, J.M., Husfeldt, Y. 1990. Palynological preparation techniques, A new macerationtanl-method and other modifications. Series C, Geological Survey of Denmark and Greenland, vol. 10, 1-23.

Poulsen, N. E. & Riding, J. B., 2003: The Jurassic dinoflagellate cyst zonation of Subboreal Northwest Europe. Geological Survey of Denmark and Greenland (GEUS) Bulletin 1, 115-144. doi: 10.34194/geusb.v1.4650

Priem, H. N. A., Mulder, F. G., Boelrijk, N. a. I. M., Hebeda, E. H., Verschure, R. H. & Verdurmen, E. a. T., 1968: Geochronological and palaeomagnetic reconnaissance survey in parts of Central and Southern Sweden. Physics of the Earth and Planetary Interiors 1, 373-380. doi: 10.1016/0031-9201(68)90033-2

Printzlau, I. & Larsen, O., 1972: K/Ar Age Determinations on Alkaline Olivine Basalts from Skåne, Southern Sweden. 94, 259-269. doi: 10.1080/11035897209454201

Salin, E., Sundblad, K. & Lahaye, Y., 2021: A 1.85 Ga volcanic arc offshore the proto-continent Fennoscandia in southern Sweden. Precambrian Research 356, 106134. doi: 10.1016/j.precamres.2021.106134

Sorgenfrei, T., Buch, A., 1964: Deep tests in Denmark, 1935–1959. Dan. Geol. Unders., 3, Raekke 36 146 p.
Svedmark, E., 1883: Mikroskopisk undersökning af dé vid Djupadal i Skåne förekommande basaltbergarterna. Geologiska Föreningen i Stockholm Förhandlingar 6, 574-582. doi: 10.1080/11035898309444104
Söderlund, P., Söderlund, U., Möller, C., Gorbatschev, R. & Rodhe, A., 2004: Petrology and ion microprobe U-Pb chronology applied to a metabasic intrusion in southern Sweden: A study on zircon formation during metamorphism and deformation. Tectonics 23, n/a-n/a. doi: 10.1029/2003tc001498
Söderlund, U. & Ask, R., 2006: Mesoproterozoic bimodal magmatism along the Protogine Zone, S Sweden: three magmatic pulses at 1.56, 1.22 and 1.205 Ga, and regional implications. GFF 128, 303-310. doi: 10.1080/11035890601284303
Tappe, S., 2004: Mesozoic mafic alkaline magmatism of southern Scandinavia. Contributions to Mineralogy and Petrology 148, 312-334. doi: 10.1007/s00410-004-0606-y
Tappe, S., Smart, K. A., Stracke, A., Romer, R. L., Prelević, D. & Van Den Bogaard, P., 2016: Melt evolution beneath a rifted craton edge: 40 Ar/ 39 Ar geochronology and Sr–Nd–Hf–Pb isotope systematics of primitive alkaline basalts and lamprophyres from the SW Baltic Shield. Geochimica et Cosmochimica Acta 173, 1-36. doi: 10.1016/j.gca.2015.10.006
Teisseyre, W., 1893: Całokształtpłyty paleozoicnej Podola galicyjskiego. Rzecz o przyszłych wierceniach głębokich na Podolu opolskim. Kosmos, Lwow 18, 310–336.
Timmerman, M. J., Heeremans, M., Kirstein, L. A., Larsen, B. T., Spencer-Dunworth, E.-A. & Sundvoll, B., 2009: Linking changes in tectonic style with magmatism in northern Europe during the late Carboniferous to latest Permian. Tectonophysics 473, 375-390. doi: 10.1016/j.tecto.2009.03.011
Tornquist, A., 1908: Die Festellung des Südwestrandes des baltischrussischen Schildes und die geotektonische Zugehörigkeit der ostpreussischen Scholle. Schr. Phys. Okonom. Ges. Konigsb. 49, 1–12.
Tornquist, A., 1910: Geologie von Ostpreussen. Gerbrüder Borntraeger, Berlin. 231 p.
Torsvik, T. H., Smethurst, M., Burke, K. & Steinberger, B., 2008: Long term stability in deep mantle structure: Evidence from the ~300 Ma Skagerrak-Centered Large Igneous Province (the SCLIP). Earth and Planetary Science Letters 267, 444-452. doi: 10.1016/j.epsl.2007.12.004
Tralau, H., 1973: En palynologisk åldersbestämning av vulkanisk aktivitet i Skåne. Fauna och Flora, 121-125.
Tullberg, S. A. & Nathorst, A. G., 1880: Meddelande om en växtlemningar innchällande basaltvacka-vid Djupadal i Skåne. Geologiska Föreningen i Stockholm Förhandlingar 5, 230-232. doi: 10.1080/11035898009444984
Ulmius, J., Möller, C., Page, L., Johansson, L. & Ganerød, M., 2018: The eastern boundary of Sveconorwegian reworking in the Baltic Shield, defined by 40Ar/39Ar geochronology across the southernmost Sveconorwegian Province. Precambrian Research 307. doi: 10.1016/j.precamres.2018.01.008
Vajda, V., Linderson, H. & Mcloughlin, S., 2016: Disrupted vegetation as a response to Jurassic volcanism in southern Sweden. Geological Society, London, Special Publications 434, 127-147. doi: 10.1144/sp434.17
Van De Schootbrugge, B., Houben, A. J. P., Ercan, F. E. Z., Verreussel, R., Kerstholt, S., Janssen, N. M. M., Nikitenko, B. & Suan, G., 2020: Enhanced Arctic-Tethys connectivity ended the Toarcian Oceanic Anoxic Event in NW Europe. Geological Magazine 157, 1593-1611. doi: 10.1017/s0016756819001262
Vejbæk, O. V., 1990: The Horn Graben, and its relationship to the Oslo Graben and the Danish Basin. Tectonophysics 178, 29-49. doi: 10.1016/0040-1951(90)90458-k
Wahlgren, C.-H., Cruden, A. R. & Stephens, M. B., 1994: Kinematics of a major fan-like structure in the eastern part of the Sveconorwegian orogen, Baltic Shield, south-central Sweden. Precambrian Research 70, 67-91. doi: 10.1016/0301-9268(94)90021-3
Wik, N.-G., Andersson, J., Bergström, U., Claeson, D., Juhojuntti, N., Kero, L., Lundqvist, L., Möller, C., Sukotjo, S. & Wikman, H., 2006: Beskrivning till regional berggrundskarta över Jönköpings län. SGU. 60 pp.
Wikman, H., BergströM, J., Sivhed, U. & Sgu, S. G. U. K., 1993: Beskrivning till berggrundskartan Helsingborg SO. Description to the map of solid rocks Helsingborg SO. SGU, Uppsala. 114 pp.
Wikman, H. & Sivhed, U., 1993: Beskrivning till berggrundskartan Kristianstad SV. Description to the map of solid rocks Kristianstad SV. Sveriges geologiska undersökning, Uppsala.

Tidigare skrifter i serien ”Examensarbeten i Geologi vid Lunds universitet”:

598. Jirdén, Elin, 2020: Kustprocesser i Arktis – med en fallstudie på Prins Karls Forland, Svalbard. (15 hp)
599. Chonewicz, Julia, 2020: The Eemian Baltic Sea hydrography and paleoenvironment based on foraminiferal geochemistry. (45 hp)
600. Paradeisis-Stathis, Savvas, 2020: Holocene lake-level changes in the Siljan Lake District – Towards validation of von Post’s drainage scenario. (45 hp)
601. Johansson, Adam, 2020: Groundwater flow modelling to address hydrogeological response of a contaminated site to remediation measures at Hjortsberga, southern Sweden. (15 hp)
602. Barrett, Aodhan, 2020: Major and trace element geochemical analysis of norites in the Hakefjorden Complex to constrain magma source and magma plumbing systems. (45 hp)
603. Lundqvist, Jennie, 2020: ”Man fyller det med information helt enkelt”: en fenomenografisk studie om studenters upplevelse av geologisk tid. (45 hp)
604. Zachén, Gabriel, 2020: Classification of four mesosiderites and implications for their formation. (45 hp)
605. Viðarsdóttir, Halla Margrét, 2020: Assessing the biodiversity crisis whitin the Triassic-Jurassic boundary interval using redox sensitive trace metals and stable carbon isotope geochemistry. (45 hp)
606. Tan, Brian, 2020: Nordvästra Skånes prekambriska geologiska utveckling. (15 hp)
607. Taxopoulou, Maria Eleni, 2020: Metamorphic micro-textures and mineral assemblages in orthogneisses in NW Skåne – how do they correlate with technical properties? (45 hp)
608. Damber, Maja, 2020: A palaeoecological study of the establishment of beech forest in Söderåsen National Park, southern Sweden. (45 hp)
609. Karastergios, Stylianos, 2020: Characterization of mineral parageneses and metamorphic textures in eclogite- to highpressure granulite-facies marble at Allmenningen, Roan, western Norway. (45 hp)
610. Lindberg Skutsjö, Love, 2021: Geologiska och hydrogeologiska tolkningar av Sky-TEM-data från Vombsänkan, Sjöbo kommun, Skåne. (15 hp)
611. Hertzman, Hanna, 2021: Odensjön - A new varved lake sediment record from southern Sweden. (45 hp)
612. Molin, Emmy, 2021: Rare terrestrial vertebrate remains from the Pliensbachian (Lower Jurassic) Hasle Formation on the Island of Bornholm, Denmark. (45 hp)
613. Höjbert, Karl, 2021: Dendrokronologi - en nyckelmetod för att förstå klimat- och miljöförändringar i Jämtland under holocen. (15 hp)
614. Lundgren Sassner, Lykke, 2021: A Method for Evaluating and Mapping Terrestrial Deposition and Preservation Potential- for Palaeostorm Surge Traces. Remote Mapping of the Coast of Scania, Blekinge and Halland, in Southern Sweden, with a Field Study at Dalköpinge Ängar, Trelleborg. (45 hp)
615. Granbom, Johanna, 2021: En detaljerad undersökning av den mellanordoviciska ”furudalkalkstenen” i Dalarna. (15 hp)
616. Greiff, Johannes, 2021: Oolites from the Arabian platform: Archives for the aftermath of the end-Triassic mass extinction. (45 hp)
617. Ekström, Christian, 2021: Rödfärgade utfällningar i dammanläggningar orsakade av G. ferruginea och L. ochracea - Problemstatistik och mikrobiella levnadsförutsättningar. (15 hp)
618. Östsjö, Martina, 2021: Geologins betydelse i samhället och ett första steg mot en geopark på Gotland. (15 hp)
619. Westberg, Märta, 2021: The preservation of cells in biomineralized vertebrate tissues of Mesozoic age – examples from a Cretaceous mosasaur (Reptilia, Mosasauridae). (45 hp)
620. Gleisner, Lovisa, 2021: En detaljerad undersökning av kalkstenslager i den mellanordoviciska gullhögenformationen på Billingen i Västergötland. (15 hp)
621. Bonnevier Wallstedt, Ida, 2021: Origin and early evolution of isopods - exploring morphology, ecology and systematics. (15 hp)
622. Selezeneva, Natalia, 2021: Indications for solar storms during the Last Glacial Maximum in the NGRIP ice core. (45 hp)
623. Bakker, Aron, 2021: Geological characteri-

sation of geophysical lineaments as part of the expanded site descriptive model around the planned repository site for high -level nuclear waste, Forsmark, Sweden. (45 hp)

624. Sundberg, Oskar, 2021: Jordlagerföljden i Höjeådalen utifrån nya borrningar. (15 hp)
625. Sartell, Anna, 2021: The igneous complex of Ekmanfjorden, Svalbard: an integrated field, petrological and geochemical study. (45 hp)
626. Juliusson, Oscar, 2021: Implications of ice-bedrock dynamics at Ullstorp, Scania, southern Sweden. (45 hp)
627. Eng, Simon, 2021: Rödslam i svenska kraftdammar - Problematik och potentiella lösningar. (15 hp)
628. Kervall, Hanna, 2021: Feasibility of Enhanced Geothermal Systems in the Precambrian crystalline basement in SW Scania, Sweden. (45 hp)
629. Smith, Thomas, 2022: Assessing the relationship between hypoxia and life on Earth, and implications for the search for habitable exoplanets. (45 hp)
630. Neumann, Daniel, 2022: En mosasaurie (Reptilia, Mosasauridae) av paleocensk ålder? (15 hp)
631. Svensson, David, 2022: Geofysisk och geologisk tolkning av kritskollors utbredning i Ystadsområdet. (15 hp)
632. Allison, Edward, 2022: Avsättning av Black Carbon i sediment från Odensjön, södra Sverige. (15 hp)
633. Jirdén, Elin, 2022: OSL dating of the Mesolithic site Nilsvikdalen 7, Bjorøy, Norway. (45 hp)
634. Wong, Danny, 2022: GIS-analys av effekten vid stormflod/havsnivåhöjning, Morupstrakten, Halland. (15 hp)
635. Lycke, Björn, 2022: Mikroplast i vattenavsatta sediment. (15 hp)
636. Schönherr, Lara, 2022: Grön fältspat i Varbergskomplexet. (15 hp)
637. Funck, Pontus, 2022: Granens ankomst och etablering i Skandinavien under postglacial tid. (15 hp)
638. Brotzen, Olga M., 2022: Geologiska besöksmål och geoparker som plattform för popularisering av geovetenskap. (15 hp)
639. Lodi, Giulia, 2022: A study of carbon, nitrogen, and biogenic silica concentrations in Cyperus papyrus, the sedge dominating the permanent swamp of the Okavango Delta, Botswana, Africa. (45 hp)
640. Nilsson, Sebastian, 2022: PFAS- En sammanfattning av ny forskning, med ett fokus på föroreningskällor, provtagning, analysmetoder och saneringsmetoder. (15 hp)
641. Jägfeldt, Hans, 2022: Molnens påverkan på jordens strålningsbalans och klimatsystem. (15 hp)
642. Sundberg, Melissa, 2022: Paleontologiska egenskaper och syreisotopsutveckling i borrkärnan Limhamn-2018: Kopplingar till klimatförändringar under yngre krita. (15 hp)
643. Bjermo, Tim, 2022: A re-investigation of hummocky moraine formed from ice sheet decay using geomorphological and sedimentological evidence in the Vomb area, southern Sweden. (45 hp)
644. Halvarsson, Ellinor, 2022: Structural investigation of ductile deformations across the Frontal Wedge south of Lake Vättern, southern Sweden. (45 hp)
645. Brakebusch, Linus, 2022: Record of the end -Triassic mass extinction in shallow marine carbonates: the Lorüns section (Austria). (45 hp)
646. Wahlquist, Per, 2023: Stratigraphy and palaeoenvironment of the early Jurassic volcaniclastic strata at Djupadalsmölla, central Skåne, Sweden. (45 hp)

LUNDS UNIVERSITET

Geologiska institutionen
Lunds universitet
Sölvegatan 12, 223 62 Lund